ICIMOD Working Paper 2013/5

ICIMOD 30

THREE DECADES
FOR MOUNTAINS AND PEOPLE

Validation of NOAA CPC_RFE Satellite-based Rainfall Estimates in the Central Himalayas

USAID
FROM THE AMERICAN PEOPLE

About ICIMOD

The International Centre for Integrated Mountain Development, ICIMOD, is a regional knowledge development and learning centre serving the eight regional member countries of the Hindu Kush Himalayas – Afghanistan, Bangladesh, Bhutan, China, India, Myanmar, Nepal, and Pakistan – and based in Kathmandu, Nepal. Globalization and climate change have an increasing influence on the stability of fragile mountain ecosystems and the livelihoods of mountain people. ICIMOD aims to assist mountain people to understand these changes, adapt to them, and make the most of new opportunities, while addressing upstream-downstream issues. We support regional transboundary programmes through partnership with regional partner institutions, facilitate the exchange of experience, and serve as a regional knowledge hub. We strengthen networking among regional and global centres of excellence. Overall, we are working to develop an economically and environmentally sound mountain ecosystem to improve the living standards of mountain populations and to sustain vital ecosystem services for the billions of people living downstream – now, and for the future.

ICIMOD gratefully acknowledges the support of its core donors: the Governments of Afghanistan, Bangladesh, Bhutan, China, India, Myanmar, Nepal, Pakistan, Austria, Norway, Switzerland, and the United Kingdom.

ICIMOD Working Paper 2013/5

Validation of NOAA CPC_RFE Satellite-based Rainfall Estimates in the Central Himalayas

Mandira Singh Shrestha
Rupak Rajbhandari
Sagar Ratna Bajracharya

International Centre for Integrated Mountain Development, Kathmandu, Nepal, May 2013

Published by
International Centre for Integrated Mountain Development
GPO Box 3226, Kathmandu, Nepal

ISBN 978 92 9115 283 4 (printed)
978 92 9115 284 1 (electronic)

Production Team
A. Beatrice Murray (Consultant editor); Amy Sellmyer (Editor); Dharma R Maharjan (Layout and design); Asha Kaji Thaku (Editorial assistant)

Printed by Quality Printers (P) Ltd, Kathmandu, Nepal

This publication is also available at www.icimod.org/publications

Citation: Shrestha, MS; Rajbhandari, R; Bajracharya, SR (2013) *Validation of NOAA CPC_RFE satellite-based rainfall estimates in the central Himalayas.* ICIMOD Working Paper 2013/5. Kathmandu: ICIMOD

Contents

List of Figures

List of Tables

Foreword

The Hindu Kush Himalayan region is vulnerable to many types of natural hazard, and especially to floods and landslides. Annually, thousands of lives are lost, infrastructure worth millions of dollars is destroyed, and large numbers of people are rendered homeless by floods. It is difficult to reduce the actual occurrence of floods, but the damage and adverse impacts can be averted or minimized with adequate warning. In order to prepare timely and accurate flood warnings, however, it is necessary to have good information about rainfall. The main method used to estimate rainfall is interpolation of measurements from a network of hydrometeorological stations. However, the number of hydrometeorological stations in the high mountain areas of the Hindu Kush Himalayas is limited as a result of the steep terrain and poor accessibility, and there is little information available about rainfall in the upper catchments of the flood-prone rivers. Advances in technology and the availability of satellite-based rainfall estimates provide an opportunity to supplement gauge-observed data with estimates and provide early warning to the people at risk in this otherwise data sparse region.

Since 2006, the International Centre for Integrated Mountain Development (ICIMOD) has been working to assess the accuracy and test the applicability of satellite-based rainfall estimates in the Hindu Kush Himalayan region in collaboration with regional partners and with technical support from the National Oceanic and Atmospheric Administration (NOAA) and United States Geological Survey (USGS) and financial support from United States Agency for International Development Office of Foreign Disaster Assistance (USAID/OFDA). In 2008, ICIMOD published the results of preliminary tests of the accuracy of rainfall estimates over the region. This publication presents the findings of a detailed assessment of the accuracy of CPC_RFE2.0 rainfall estimates over the central Himalayas of Nepal. The results indicate that the spatial detection and trends are overall good, and with appropriate bias correction, the data could be applied in flood forecasting.

Reducing vulnerability and building the resilience of communities in the region to extreme weather events remains a priority for ICIMOD as it embarks on its Medium Term Action Plan for 2013-2017. ICIMOD and its partners are committed to work together on disaster risk reduction and minimize the adverse impacts of disasters. We hope that this publication will contribute further to this work.

David Molden
Director General, ICIMOD

Acknowledgements

ICIMOD is grateful to the United States Agency for International Development Office of Foreign Disaster Assistance (USAID/OFDA) for funding this project. Our special thanks go to A Sezin Tokar, Hydrometeorological Hazard Advisor, USAID/OFDA, for her encouragement and valuable support during the study. We would like to express our gratitude to the resource people from the National Oceanic and Atmospheric Administration (NOAA) and United States Geological Survey (USGS) for their technical support, in particularly Wassila Thiaw, Vadlamani B. Kumar, Eric Wolvovsky, Tim Love, and Guleid Artan. We thank the Department of Hydrology and Meteorology (DHM) Nepal for providing the data for the study and for their valuable contributions. Finally, the authors would like to thank all those in ICIMOD who contributed to the success of the project and the preparation of the publication itself.

Acronyms and Abbreviations

AFN	Asian Flood Network
AMSU-B	Advanced Microwave Soundin Unit
DHM	Department of Hydrology and Meteorology
ETS	equitable threat score
FAR	false alarm ratio
GeoSFM	Geospatial Streamflow Model
GPI	Geostationary Operational Environmental Satellite Precipitation Index
GSMaP	Global Satellite Mapping Precipitation
GTS	Global Telecommunications System (WMO)
HKH	Hindu Kush Himalayan region
IR	infrared
MAE	mean absolute error
NOAA	National Oceanic and Atmospheric Administration
OFDA	Office of Foreign Disaster Assistance
PE	percentage error
POD	probability of detection
RSME	root mean square error
SRE	satellite rainfall estimates
SSMI	spcial sensor microwave imager
USAID	United States Agency for International Development
USGS	United States Geological Survey
WMO	World Meteorological Organization

Introduction

Background

Flood early warning systems are one of the most effective ways to minimize the loss of life and property. It is very important to have a reliable flood forecasting system as a basis for establishing a reliable early warning system which can be transmitted down to the community in order to minimize the impact of flood disasters. Precipitation is highly variable in both space and time and is an important input in rainfall runoff modelling. The amount of rainfall and its spatial distribution are important factors in meteorology, climatology, and hydrology. Accurate rainfall estimations are essential for timely flood forecasting and warning. In many regions, operational flood forecasting has traditionally relied upon a dense network of rain gauges or ground-based rainfall measuring radars that report in real time. Flood forecasting in basins with sparse or non-existent rain gauges poses an additional challenge. In such areas, satellite rainfall estimates (SRE) could provide information on rainfall occurrence, amount, and distribution (Adler et al. 2003; Hong et al. 2007; Shrestha et al. 2008 a,b) and be used for hydrological modelling to predict floods.

The availability of global coverage of satellite data offers an effective and economical means of calculating areal rainfall estimates in sparsely gauged areas (Artan et al. 2007). Several high resolution global satellite-based rainfall products are currently available from various operational agencies, as well from research and academic institutions (Ebert et al. 2007; Huffman et al. 2007; Kubota et al. 2009). For example, satellite algorithms like the Global Satellite Mapping Precipitation (GSMaP) (Ushio et al. 2009), CPC_RFE2.0 (Xie et al. 2002), and CMORPH (Joyce et al. 2004) are currently available at a spatial resolution of 0.1 degrees or higher and a temporal resolution of 24 hours or less. The availability of high resolution satellite-based products at a finer temporal (hourly and daily) and spatial (0.1°) resolution provides an opportunity to apply rainfall estimates for timely flood forecasts in data sparse regions. However, satellite-based rainfall data have uncertainty and, when applied in rainfall runoff models for flood simulation, this uncertainty has an effect on the accuracy of the predictions. Thus the satellite rainfall estimates need to be validated against rain gauge measurements to gain an idea of their accuracy and expected error characteristics in various applications before they can be used in modelling. Figure 1 shows an example of a daily satellite-based rainfall estimate for the Hindu Kush Himalayan (HKH) region provided by the National Oceanic and Atmospheric Administration (NOAA) Climate Prediction Centre (CPC) CPC_RFE2.0 (www.cpc.ncep.noaa.gov/products/fews/SASIA/rfe.shtml).

Following the successful validation of satellite rainfall estimates for regions in Africa, and similar estimates made over other parts of the world (Kidd 2005; Laurent et al. 1998; Vila et al. 2003; Dinku et al. 2008), the CPC_RFE2.0 system is now being tested in South Asia (Shrestha et al. 2008 a,b). The present study focuses on the verification of rainfall by CPC_RFE2.0 satellite-based rainfall estimates over the whole of Nepal.

The ICIMOD Satellite Rainfall Estimation Project

ICIMOD has collaborated with regional partner countries since 2001 on flood disaster mitigation, with support from the United States Agency for International Development Office of Foreign Disaster Assistance (USAID/OFDA). ICIMOD shared 24-hour, 48-hour, and 72-hour rainfall forecasts made available by OFDA for the HKH region with all its partners during the monsoon of 2004. Partners' interest and requests led to a long-term project 'Application of Satellite Rainfall Estimates in the Hindu Kush Himalayan Region' on satellite rainfall verification and application. As part of the project, a series of trainings and workshops were held under the Asia Flood Network (AFN) programme of USAID/OFDA with technical support from NOAA and the United States Geological Survey (USGS).

Phase I of the project ended in June 2008, and Phase II, which continued the validation of the satellite-based rainfall estimates over the Himalayan region, ended in June 2010. The project engaged government representatives of national hydrological and meteorological services, and organizations involved in flood disaster management,

Figure 1: **CPC_RFE2.0 satellite rainfall estimate for South Asia** (daily accumulation in mm, October 01 2012)

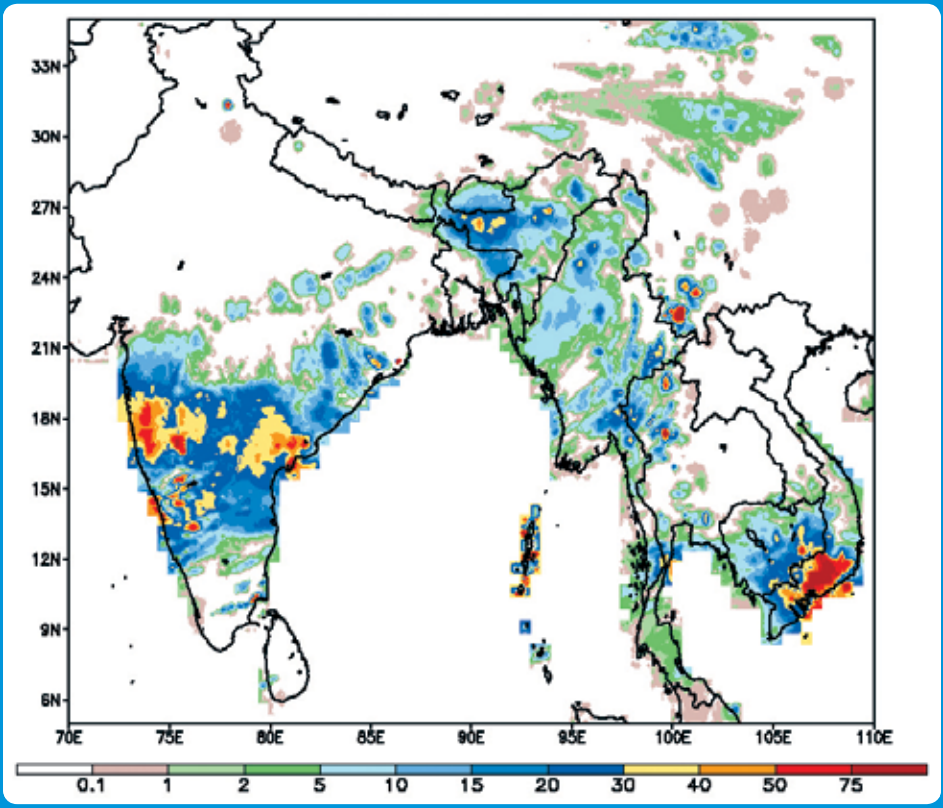

in each of the participating countries. It fostered discussion and dialogue between the participating countries and contributed towards strengthening the capacities of partner institutions in applying satellite rainfall estimates for flood forecasting.

The project aimed to minimize the loss of lives and property by reducing the region's vulnerability to floods and droughts – in particular in the Indus and Ganges-Brahmaputra-Meghna basins. The project sought to strengthen regional cooperation in flood forecasting and information exchange, and build capacity among the partner institutions. The main objective was to validate the CPC_RFE2.0 satellite rainfall estimates for the HKH region in order to determine their operational viability and improve the algorithm, and to apply rainfall estimates to USGS's Geospatial Streamflow Model (GeoSFM).

Present Study

The project carried out quantitative validation of the CPC_RFE2.0 product based on independent ground station data at national and regional levels. The objectives of the part of the study described in this publication were to validate the CPC_RFE2.0 over the central Himalayas of Nepal and assess the accuracy of the estimates. The study assessed the accuracy of the satellite-based rainfall estimates on a daily, monthly, seasonal, and annual basis and investigated how the NOAA CPC_RFE2.0 satellite rainfall product performs over Nepal.

The report is divided into five chapters, followed by an annex. This first chapter introduces the project and its objectives. Chapter Two describes the study area and data used for the study. Chapter Three presents the procedures and techniques for validating NOAA's SRE products in the study area, including data preparation, data quality control, data conversion, methods of interpolation, and the statistical measures used to compare the satellite estimates with rain-gauge data. Chapter Four presents the results and discussion. Finally, Chapter Five summarizes the conclusions and suggests a way forward.

Study Region and Data

Study Region

Nepal is a predominantly mountainous country with a total area of 147,181 km^2 covering five physiographic regions: the Terai, Siwalik, Middle Mountains, High Mountains, and Himal. The elevation varies from 60 m in the south to 8,848 m in the north within a short horizontal distance of less than 200 km. Water-induced disasters are very prevalent and annually many lives are lost and property worth millions of dollars is destroyed. Due to the diverse geological setting, rugged terrain, and monsoon precipitation, Nepal is prone to floods, landslides, and glacial lake outburst floods (GLOF). The dominant rainfall season is the monsoon, which runs from June to September; 80 per cent of the annual rainfall falls during this period. The UNDP global report on reducing disaster risk (UNDP 2004) cites Nepal as having a high vulnerability for flood disasters based on 20 years of data (1980-2000). Between 1983 and 2005, an average of 309 people lost their lives annually in Nepal due to floods and landslides, accounting for over 60 per cent of those who died due to different types of disasters in the country (Khanal et al. 2007). The high level of poverty and rate of population growth has further increased the vulnerability to flood disasters.

Nepal has relatively few ground-based rain gauges, on average one gauge per 331 km^2,according to the Department of Hydrology and Meteorology (DHM), with very few in the mountainous areas. Due to the limited spatial coverage of ground based gauges, lack of real-time rainfall data, and constraints in technical and financial resources, operational flood forecasting has yet to be initiated (Shrestha et al. 2008a). SRE may be an appropriate approach for Nepal to predict and forecast rainfall-induced runoff that may produce flooding.

Data Availability

NOAA CPC_RFE2.0 rainfall estimates

The Climate Prediction Center (CPC) of NOAA has produced daily precipitation estimates (CPC_RFE2.0) on a 0.1 degree latitude/longitude grid over the HKH region (60°E-110°E; 5°N-40°N) in near real-time, at a spatial resolution of 0.1° by 0.1° (Xie et al. 2002) since 2001. The initial version, CPC_RFE1.0, was operational from 1996 to 2000 over Africa. The input data used for the operational rainfall estimates are from a combination of satellite estimates and rain gauges that use the algorithm developed by Xie and Arkin (1996). The satellite input data are from three sources: Advanced Microwave Sounding Unit (AMSU-B) microwave satellite precipitation estimates up to four times per day; Special Sensor Microwave Imager (SSMI) satellite rainfall estimates up to four times per day; and Geostationary Operational Environmental Satellite Precipitation Index (GPI) cloud-top infrared (IR) temperature precipitation estimates on a half-hourly basis. The rain gauge data are from the Global Telecommunications System (GTS) of the WMO. The three satellite estimates are first combined linearly using predetermined weighting coefficients then merged with station data to determine the final rainfall. The shape of the precipitation is given by the combined satellite estimates, and the magnitude is inferred from GTS station data. The merging technique using satellite-based rainfall data and ground gauge data increases the accuracy of the rainfall estimates by reducing significant bias and random error compared to individual data sources. Before these estimates can be used in modelling, however, they must be tested and optimized to ensure that they really reflect the situation on the ground. This system has produced an automatic rainfall analysis in South Asia since May 2001. Six years (2002 to 2007) of 24-hour CPC_RFE2.0 gridded rainfall data of 0.1° by 0.1° were obtained over the HKH region.

Gauge-observed rainfall

The daily gauge-observed rainfall data for the period 2002 to 2007 from 269 stations in Nepal were provided by the Department of Hydrology and Meteorology. The distribution of the rain gauges is shown in Figure 2. The density of rainfall stations in Nepal is relatively high compared to other countries in the region. However, the distribution is uneven and very sparse in the northern mountain areas. Most stations are concentrated in urban and middle mountain areas where accessibility is easy. The rain gauge stations are listed in the Annex with details of their location and elevation.

Figure 2: **Distribution of rainfall stations in Nepal**

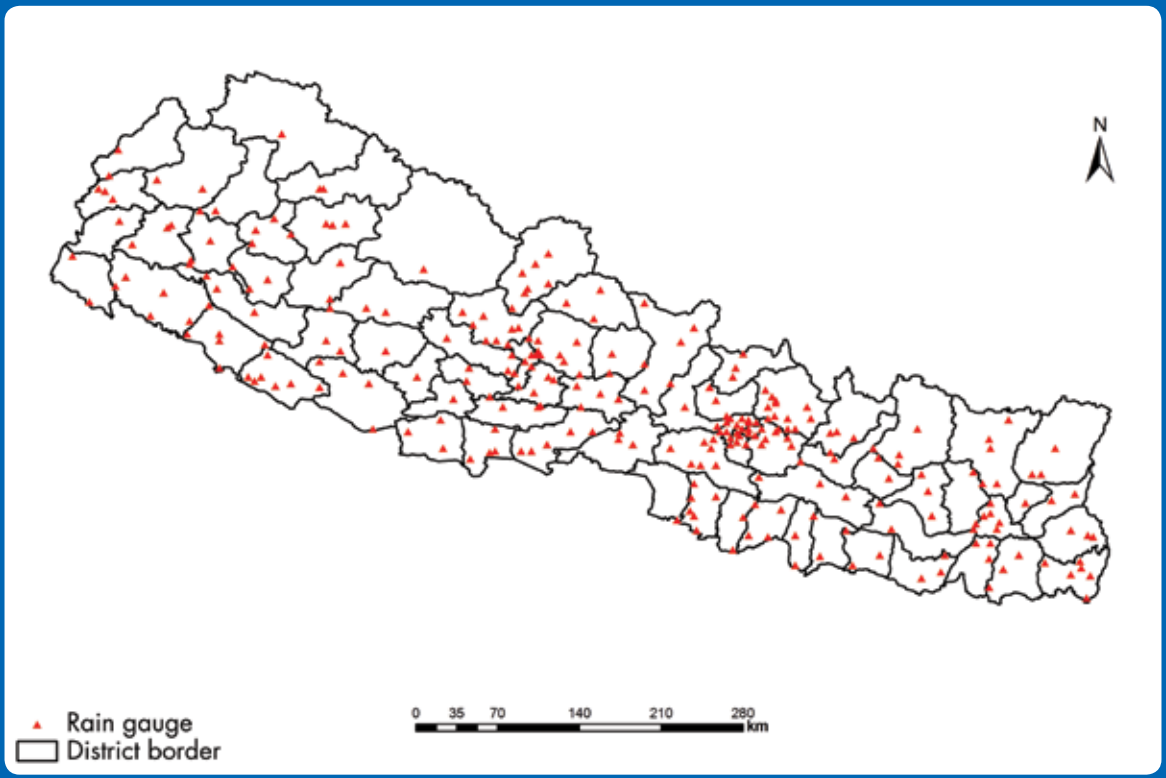

Methodology for Rainfall Verification

The methodology for SRE verification was developed based on a review of the literature on validation conducted for similar projects in other regions.

Interpolation of Gauge-Observed Rainfall

For the validation of satellite-based estimates of rainfall, the reference values must represent space-averaged rainfall values. Since the rainfall measurements are taken from a rain-gauge network, an interpolation scheme has to be used to obtain areal rainfall from the scattered point values. For the present analysis, ordinary kriging was used for interpolation. The kriging spatial interpolation method found best suitable in the Indian Himalayan region (Basistha et al. 2007) was used to convert the daily point gauge-observed rainfall data to a 0.1 degree latitude/longitude grid. This interpolated gauge-observed gridded rainfall was used as the 'ground truth' for subsequent analysis.

Kriging, a geostatistical method, is an optimal interpolation based on regression against observed (values rainfall measured) from surrounding data points, weighted according to spatial covariance values. All interpolation algorithms (inverse distance squared, splines, radial basis functions, triangulation, and others) estimate the value at a given location as a weighted sum of data values at the surrounding locations. Almost all assign weights according to functions that give a decreasing weight with increasing separation distance. Kriging assigns weights according to a (moderately) data-driven weighting function, rather than an arbitrary function, but it is still just an interpolation algorithm and will give very similar results to other methods in many cases (Isaaks and Srivastava 1989; Clark 2001). The weights attributed to different observations depend on the variability structure of the rainfall field. This variability structure is taken into account using the variogram function. The variogram is a quantitative descriptive statistic that can be graphically represented in a manner which characterizes the spatial continuity (i.e., roughness) of a data set. An empirical variogram is calculated using observed datasets and a variogram model is fitted using 'SURFER' software. This was also done using the Geostatistical tool in ArcGIS. Figure 3 shows the empirical variogram calculated for monthly data from 2002 to 2007 for Nepal.

Figure 3: **Empirical variogram used for the study**

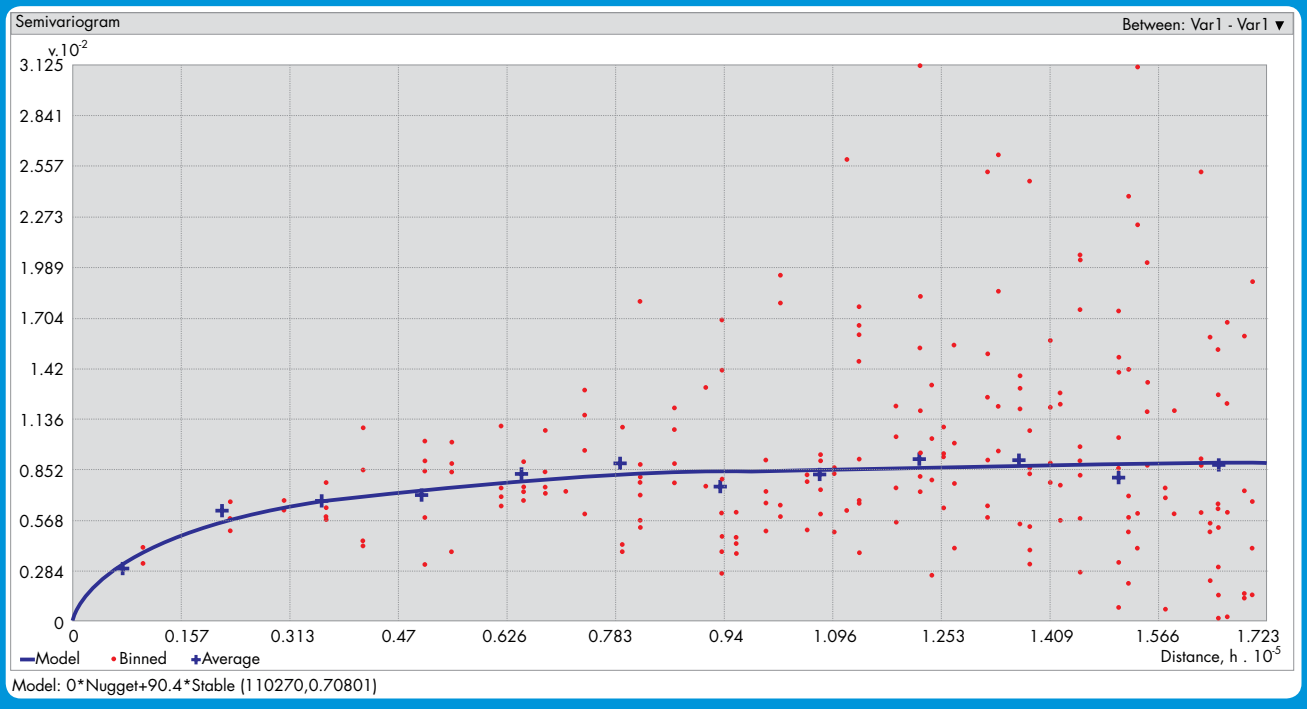

Rainfall Verification Methodology

Many methods of spatial verification are available for comparing rain gauge measurements with remotely-sensed rainfall measurements. In this study, the statistical measures used to compare the satellite estimations with the ground truth data (rain gauge) were taken from the results of the 3rd Algorithm Intercomparison Project of the Global Precipitation Climatology Project (Ebert 1996: Ebert et al. 2007). The spatial verification methods described here include visual verification, continuous statistics, and categorical statistics. The verification methodology selected in this study was based on 24-hour, monthly, seasonal, and annual accumulation rain gauge data and satellite-estimated data.

Visual Analysis

Visual verification compares maps of satellite estimates and observations. Gridded observation (independent rain-gauge data) and estimated CPC_RFE2.0 data were remapped to the same projection with the same colour scale to show the spatial distribution of rainfall (bias map). This method is not quantitative but subjective.

Continuous Verification Statistics

Continuous verification statistics measure the accuracy of a continuous variable such as rain amount or intensity. These are the most commonly used statistics in validating satellite-based estimates; many people are familiar with them and find them easy to estimate. The mean error (bias) measures the average difference between the estimated and observed values averaged over the data set. The mean absolute error (MAE) measures the average magnitude of the error. The root mean square error (RMSE) also measures the average error magnitude, but gives greater weight to larger errors (Vila et al. 2003; Vila and Lima 2006). The percentage error (PE) is the difference between estimated and observed values. The multiplicative bias is the ratio of estimated to observed rainfall values.

$$\text{Mean error} = \frac{1}{N}\sum_{i=1}^{N}(Si - Gi)$$

$$\text{Mean absolute error} = \frac{1}{N}\sum_{i=1}^{N}|Si - Gi|$$

$$\text{Root mean square error} = \sqrt{\frac{1}{N}\sum_{i=1}^{N}(Si - Gi)^2}$$

$$\text{Correlation coefficient (r)} = \frac{\sum_{i=1}^{N}(Si - \overline{S})(Gi - \overline{G})}{\sqrt{\sum_{i=1}^{N}(Si - \overline{S})^2}\sqrt{\sum_{i=1}^{N}(Gi - \overline{G})^2}}$$

$$\text{Percentage error (PE)} = \frac{estimated - observed}{observed} \times 100\%$$

$$\text{Multiplicative bias} = \frac{\frac{1}{N}\sum_{i=1}^{N}Si}{\frac{1}{N}\sum_{i=1}^{N}Gi}$$

where, Si is the satellite-estimated value at grid cell or point i, Gi is the observed ground rain gauge value at grid cell or point i, N is the number of observed samples, and $\overline{G}$ and $\overline{S}$ are the average values.

Categorical Verification Statistics

Categorical verification statistics measure the correspondence between the estimated and observed occurrence of events and is a qualitative indicator. Most are based on a 2 x 2 contingency table of yes/no events, such as rain/no rain, as shown in Table 1. The probability of detection

Table 1: **2 x 2 Contingency table**

		Estimated rainfall (SRE)	
		No rain (no)	Rain (yes)
Observed rainfall (ground rain gauge)	No rain (No)	Q1 (correct negatives)	Q2 (false alarms)
	Rain (Yes)	Q3 (misses)	Q4 (hits)

(POD) measures the fraction of observed events that was diagnosed correctly and is sometimes called the 'hit rate'. The false alarm ratio (FAR) gives the fraction of diagnosed events that were actually non-events (Ebert et al. 2007). The POD and FAR should always be used together. These and other measures are described in more detail below (based on information from www.cawcr.gov.au/projects/verification/).

Rain/no rain contingency table: The off-diagonal elements in the table characterize the error. The elements in the table (hits, misses, false alarms, correct negatives) give the joint distribution of events, while the elements above and to the right (observed yes, observed no, others) are called the marginal distributions. In the table, correct negatives (Q1) represent correctly estimated no rain events, false alarms (Q2) represent when rain was estimated by satellite but did not occur on the ground, misses (Q3) represent when rain was not estimated by satellite but did occur on the ground, and hits (Q4) represent correctly estimated rain events, where both satellite estimates and rain gauges show rain. The contingency table is a useful way to see what types of errors are being made. A perfect estimate system would produce only hits and correct negatives and no misses or false alarms. Basic statistics are used to provide information on rain identification through contingency tables taken together with conditional rain rates (0 or 1 mm/day rain/no rain thresholds). This type of table was used to measure the skill of the rainfall estimations in pinpointing rain where rain was observed on the ground.

$$\text{Probability of detection (POD)} = \frac{Q4}{Q3 + Q4} \text{ or } = \frac{hits}{hits + misses}$$

The POD is sensitive to hits, but ignores false alarms. It is very sensitive to the climatology of the region and is good for rare events. It can be artificially improved by issuing more 'yes' estimates to increase the number of hits. It should be used in conjunction with the false alarm ratio. POD is also an important component of the relative operating characteristic (ROC) used widely for probability estimates. It ranges from 0 to 1; the perfect score is 1.

$$\text{False alarm ratio (FAR)} = \frac{Q2}{Q2 + Q4} \text{ or } = \frac{false\ alarms}{hits + false\ alarms}$$

The FAR is sensitive to false alarms, but ignores misses. It is very sensitive to the climatological frequency of the event and should be used in conjunction with the probability of detection. It ranges from 0 to 1; the perfect score is 0.

In Phase 1, the study focused only on POD and FAR. These categorical statistics are affected by the climatology of the study region and might not be useful for comparing rain detection accuracy over two different climatic regions, for example the higher Himalayan and Siwalik regions. Therefore in Phase 2, a rigorous and optimum analysis was carried out to obtain significant results and some additional measurements were added to the categorical verification statistics such as the threat score (TS) and equitable threat score (ETS). These are not affected as much by wetness or dryness of the regions, thus this type of comparison is good for regional or general climatology.

$$\text{Threat score (TS)} = \frac{hits}{hits + misses + false\ alarms}$$

The TS measures the fraction of observed and/or estimated events that were correctly estimated. It can be thought of as the accuracy after correct negatives have been removed, in other words TS is only concerned with estimates that count. TS is sensitive to hits and penalizes both misses and false alarms. It does not distinguish the source of estimated error. TS does depend on the climatological frequency of events, with poorer scores for rarer events since some hits can occur due to random chance. It ranges from 0 to 1; the perfect score is 1; 0 indicates no skill.

$$\text{Equitable threat score (ETS)} = \frac{hits - hits_{random}}{hits + misses + false\ alarms - hits_{random}}$$

where

$$hits_{random} = \frac{(hits + misses)(hits + fale\ alarms)}{Total}$$

The ETS measures the fraction of observed and/or estimated events that were correctly predicted, adjusted for hits associated with random chance (for example, it is easier to correctly estimate rain occurrence in a wet climate than in a dry climate). The ETS is often used in the verification of rainfall in numerical weather prediction models because its 'equitability' allows scores to be compared more fairly across different regimes. It is sensitive to hits. It penalizes both misses and false alarms in the same way and thus does not distinguish the source of estimated error. It ranges from -1/3 to 1; the perfect score is 1, 0 indicates no skill.

Analysis and Results

The SRE were evaluated at various temporal scales: daily, monthly, seasonal, and annual. The results of the comparison of satellite-estimated and gauge-observed data are summarized below.

Comparison of Quantitiative Rainfall Distribution

Daily rainfall distribution as estimated from CPC_RFE2.0

A comparison was made of the rainfall distribution in the six years from 2002 to 2007. In the visual analysis, two kinds of comparison were made:

- Grid-to-grid comparison – in this method, all the grids lying within the country boundary are considered
- Point-to-point comparison – in this method, only those grids which have at least one rain-gauge (point data) are considered. The location of grids with one or more stations is shown in Figure 4. The grids are categorized according to the station elevation.

Figure 4: **Location of grids with one or more gauge station**

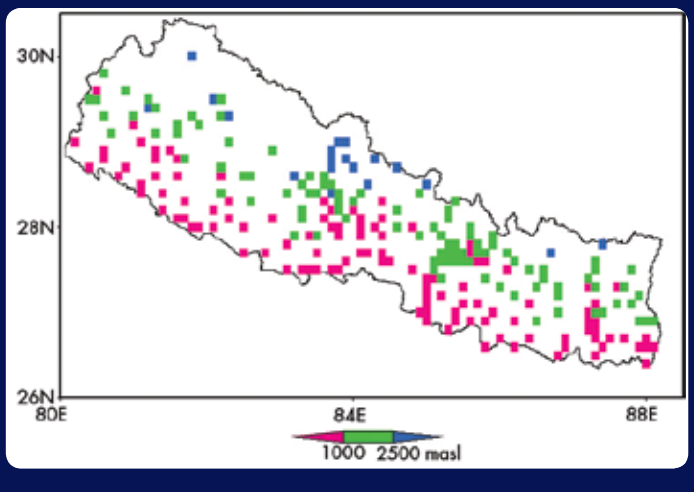

Figure 5 shows the time series of satellite-estimated (CPC_RFE2.0) and observed (rain gauge) daily rainfall for each year from 2002 to 2007 using grid-to-grid comparison. Qualitatively, the rainfall events generally match. Quantitatively, the CPC_RFE2.0 tends to substantially underestimate, but there are also some events where the CPC_RFE2.0 is greater than the observed value. The CPC_RFE2.0 overestimates are mostly during cooler months and when rainfall is low or moderate. In the rainy season, the difference between the two is more evident.

Figure 6 shows the same comparison using the point-to-point method. The underestimation by SRE is more evident, although there is little quantitative difference between the graphs prepared by the two methods.

Monthly rainfall distribution as estimated from CPC_RFE2.0

The monthly accumulated gauge-observed and satellite-estimated rainfall totals for the whole country (all grids) for each year from 2002 to 2007 are given in Tables 2 and 3 and shown in graph format in Figure 7 (grid-to-grid comparison). The data using only those grids that have a gauge station is given in Tables 4 and 5 and shown in graph format in Figure 8 (point-to-point comparison).

The differences between the observed and satellite-estimated data become clearer when the data is presented in monthly form. During the low rainfall months from October to April, the CPC_RFE2.0 estimation exhibits good results close to those of the observed data. In the higher rainfall months from May to September, it tends to underestimate, with significant underestimation in the main monsoon months which have more than 70 per cent of the annual total rainfall. The grid-to-grid comparison shows a total average annual rainfall deficiency for 2002 to 2007 of 627 mm, of which 548 mm occurs during the monsoon season. The point-to-point comparison shows slightly higher total rainfall values, both for observed rainfall (1,798 mm compared to 1,680 mm) and for the satellite estimates (1,104 mm compared to 1,054 mm). The annual rainfall deficiency using the satellite estimates is also slightly, but not significantly, higher: 695 mm, of which 587 mm occurs during the monsoon season. As the differences were not significant, only grid-to-grid comparisons were used for spatial maps and further analysis.

Figure 5: **Daily rainfall (in mm) as observed by rain gauge and satellite estimated for 2002 to 2007 using grid-to-grid comparison**

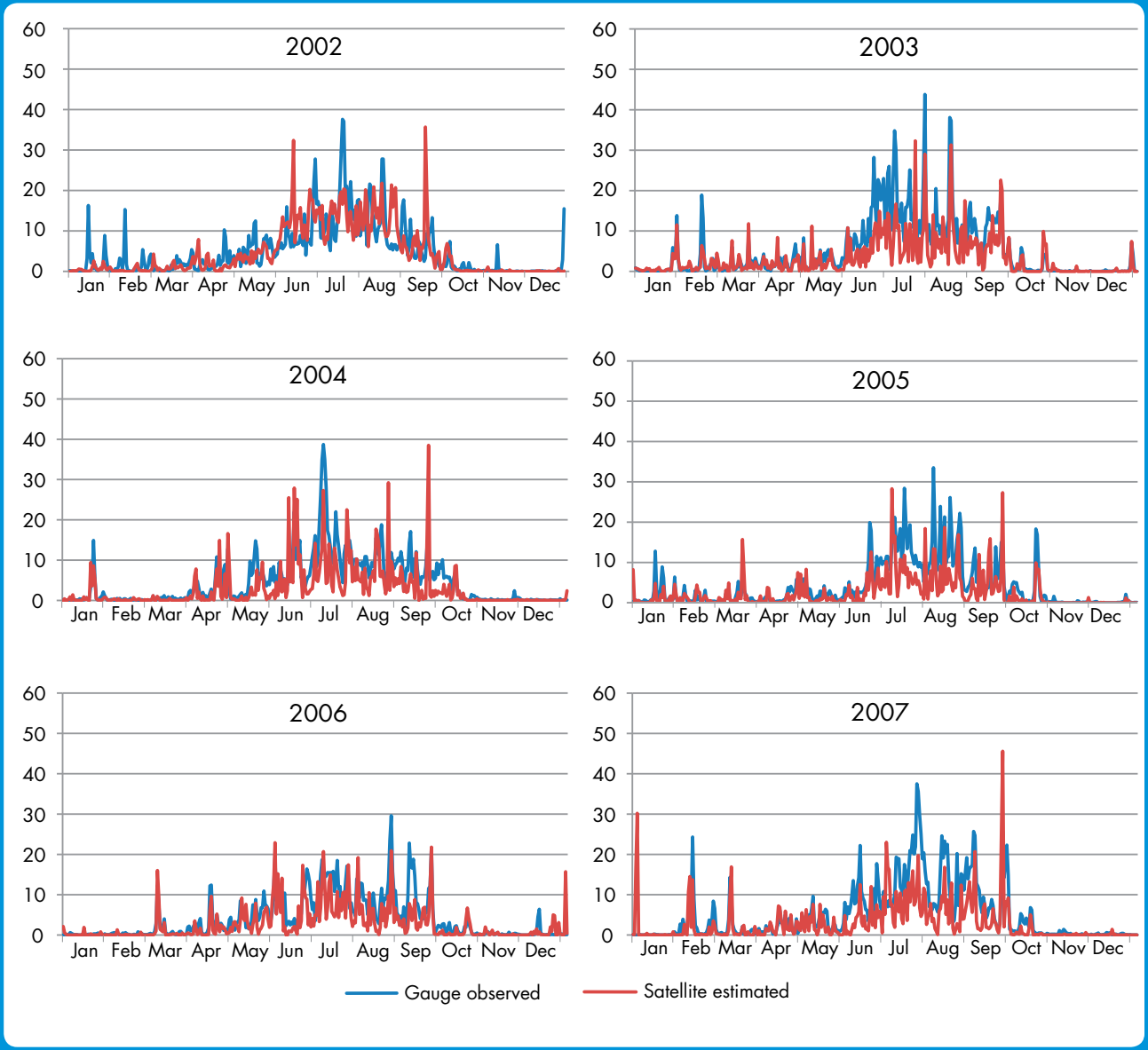

Table 2: **Observed (OBS) monthly total rainfall for 2002 to 2007, all grids**

Year	Jan	Feb	Mar	Apr	May	Jun	Jul	Aug	Sep	Oct	Nov	Dec	Total
2002	53	45	40	72	162	243	492	370	207	35	10	21	**1,748**
2003	32	54	51	58	79	337	519	380	294	33	2	15	**1,854**
2004	38	5	13	105	135	238	489	303	239	86	8	3	**1,661**
2005	57	28	40	44	70	172	404	400	184	90	5	5	**1,497**
2006	5	7	42	76	147	237	355	306	233	40	8	15	**1,470**
2007	2	94	52	59	104	256	517	378	326	51	8	5	**1,851**
Average	**31**	**39**	**39**	**69**	**116**	**247**	**462**	**356**	**247**	**56**	**7**	**11**	**1,680**

Figure 6: **Daily rainfall (in mm) as observed by rain gauge and satellite estimated for 2002 to 2007 using point-to-point comparison**

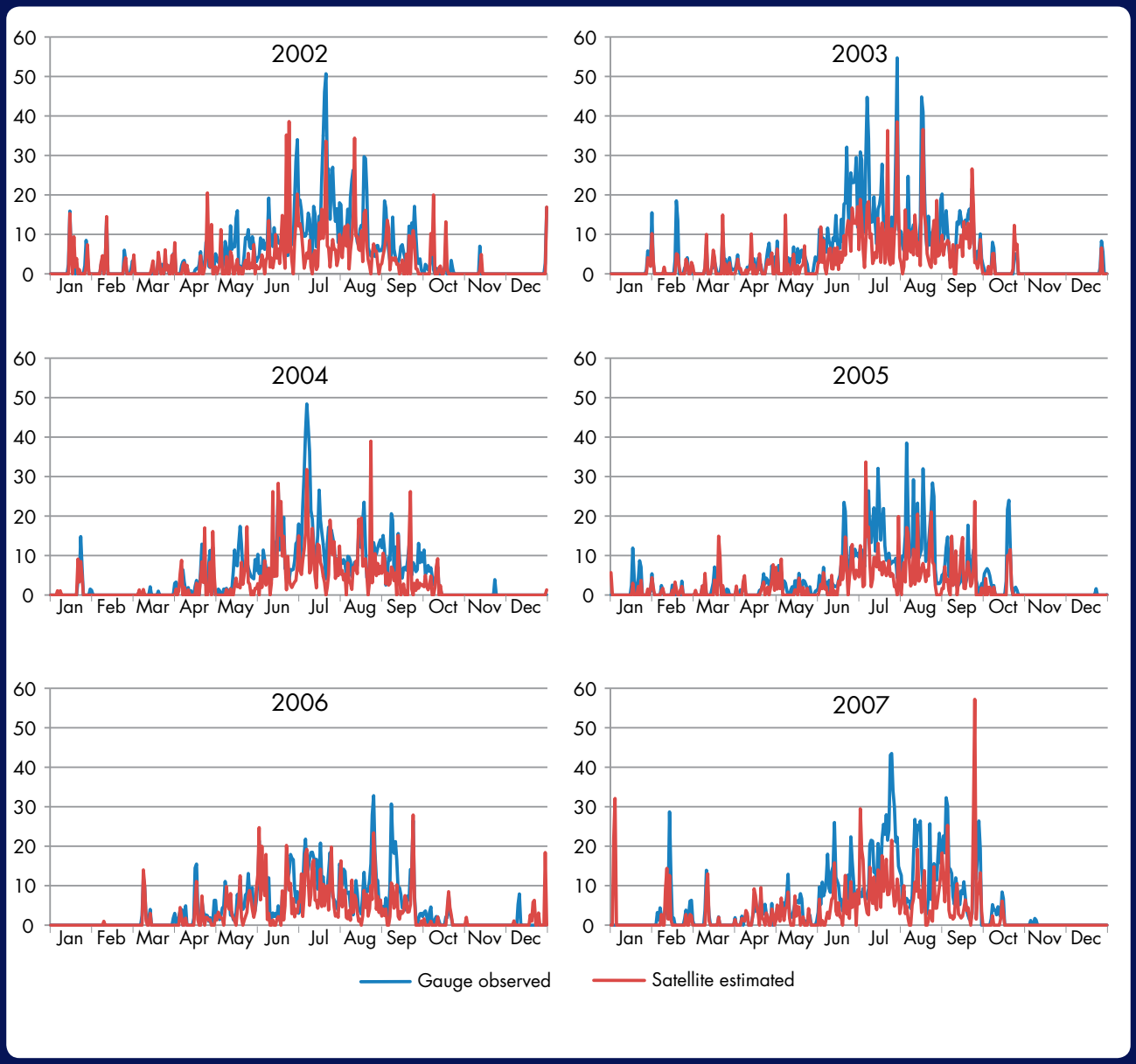

Table 3: **Satellite-estimated (SRE) monthly total rainfall for 2002 to 2007, all grids**

Year	Jan	Feb	Mar	Apr	May	Jun	Jul	Aug	Sep	Oct	Nov	Dec	Total
2002	53	52	52	71	73	181	186	239	119	81	13	20	1,141
2003	33	43	58	55	57	165	290	245	209	39	3	11	1,209
2004	34	4	5	82	62	191	267	216	143	45	1	3	1,056
2005	35	28	48	34	43	90	231	174	142	43	2	2	871
2006	6	3	36	43	100	177	247	183	122	25	7	37	986
2007	49	52	43	58	69	103	292	168	208	15	2	2	1,062
Average	**35**	**30**	**41**	**57**	**67**	**151**	**252**	**204**	**157**	**41**	**5**	**13**	1,054

Figure 7: **Monthly total rainfall (in mm) as observed by rain gauge and satellite estimated for 2002 to 2007 using grid-to-grid comparison**

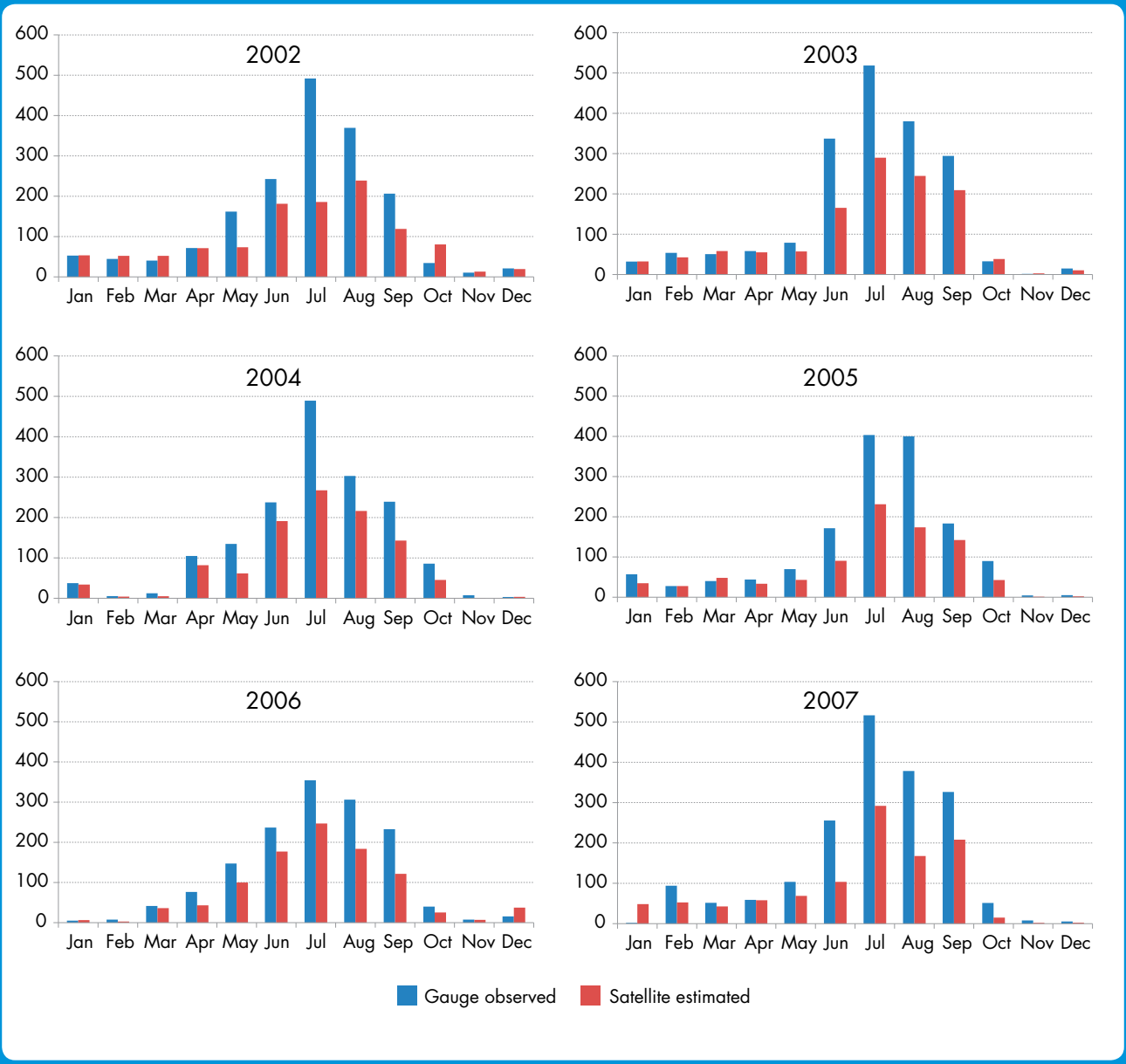

Table 4: **Observed (OBS) monthly total rainfall for 2002 to 2007, grids with stations**

Year	Jan	Feb	Mar	Apr	May	Jun	Jul	Aug	Sep	Oct	Nov	Dec	Total
2002	46	30	30	70	186	281	572	385	215	32	7	20	**1,874**
2003	29	46	47	61	83	385	578	400	315	34	0	16	**1,992**
2004	32	0	4	106	151	273	561	316	276	78	4	0	**1,801**
2005	46	12	37	46	77	191	417	440	179	107	0	2	**1,553**
2006	0	0	33	84	172	259	368	328	268	43	0	13	**1,569**
2007	0	95	38	64	111	298	576	399	376	42	4	0	**2,002**
Average	**26**	**30**	**32**	**72**	**130**	**281**	**512**	**378**	**272**	**56**	**3**	**8**	**1,798**

Figure 8: **Monthly total rainfall (in mm) as observed by rain gauge and satellite estimated for 2002 to 2007 using point-to-point comparison**

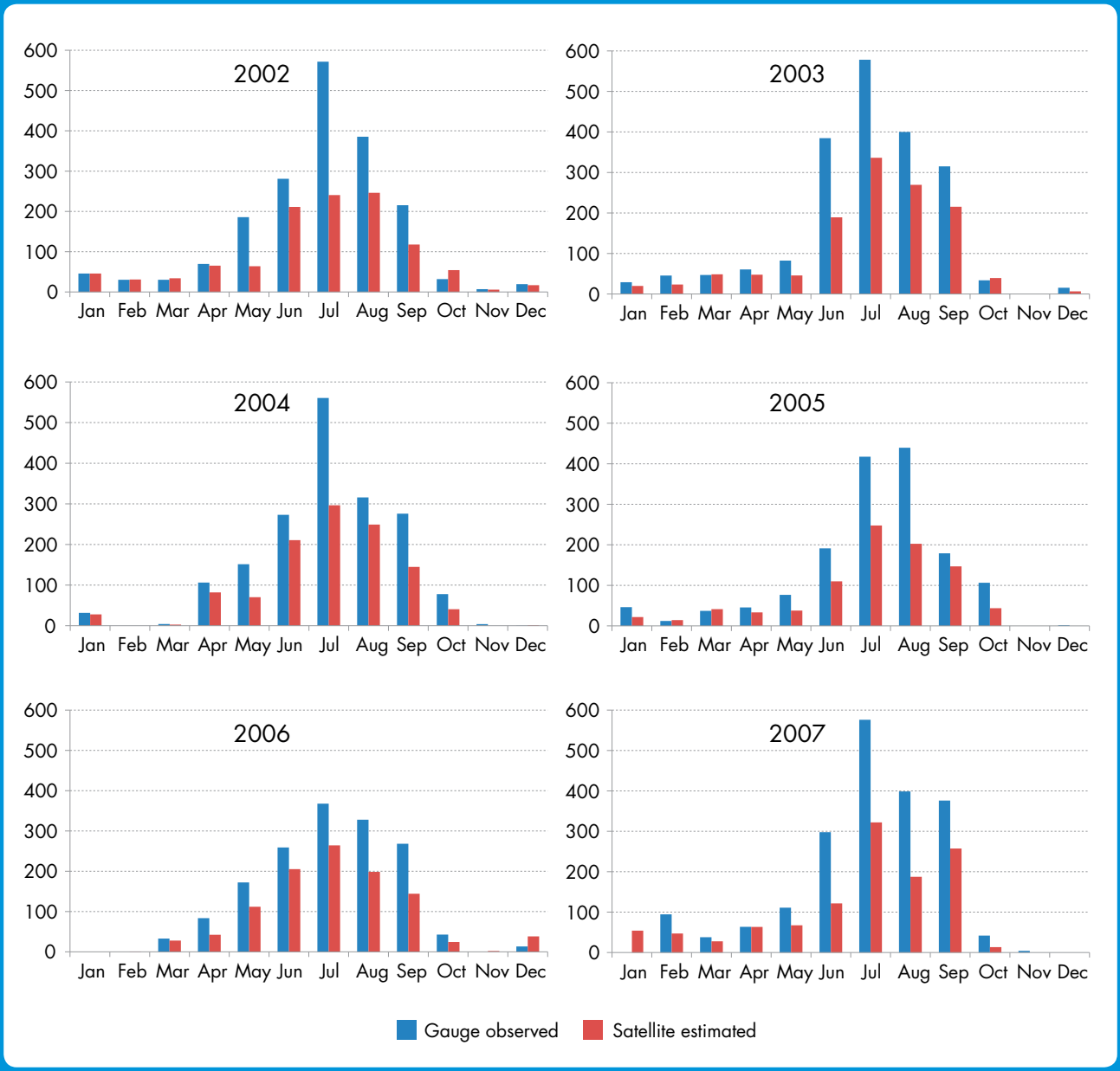

Table 5: **Satellite-estimated (SRE) monthly total rainfall for 2002 to2007, grids with stations**

Year	Jan	Feb	Mar	Apr	May	Jun	Jul	Aug	Sep	Oct	Nov	Dec	Total
2002	46	31	34	65	64	211	241	246	118	54	6	17	1,133
2003	20	23	49	48	46	189	336	269	215	39	0	7	1,242
2004	28	0	3	82	70	211	297	249	145	41	0	1	1,126
2005	22	14	41	33	38	110	248	203	147	44	0	0	899
2006	0	1	28	43	112	205	264	199	144	25	2	38	1,061
2007	54	47	28	63	67	122	322	187	257	13	0	0	1,162
Average	**28**	**19**	**30**	**56**	**66**	**175**	**285**	**226**	**171**	**36**	**1**	**11**	1,104

Seasonal distribution of rainfall as estimated from CPC_RFE2.0

The values of the gauge-observed (OBS) and satellite-estimated (SRE) seasonal rainfall totals for each year from 2002 to 2007 (all grids) are given in Table 6, together with the seasonal means for the whole period. Figure 9 shows the seasonal totals in graph format. Most of the rain falls during the monsoon season (June to September) which had 78 per cent of the observed and 72 per cent of the satellite-estimated rainfall over the whole period. In the winter season (December-January-February), the satellite estimates are close to the observed values; in the pre-monsoon (March-April-May) and post-monsoon (October-November) seasons, the satellite estimates are generally somewhat lower than the observed values; and in the monsoon (June-July-August-September) season, the satellite estimates are far lower than the observed values, on average by 548 mm.

Comparison of Spatial Distribution of Rainfall as Estimated from CPC_RFE2.0 and Gauge-Observed Data

Even when one-dimensional statistics for two data sets are very similar, the spatial continuity may be quite different. The statistical analysis provides information on descriptive statistics such as the mean, mode, correlation, and mean error. Spatial analysis provides additional information on the spatial variation. The spatial distribution of rainfall is very important for applications in meteorology, hydrology, and other environmental sciences. One of the main objectives of using the CPC_RFE2.0 estimated rainfall data is to apply it in flood forecasting and warning using a hydrological flood forecasting model; thus spatial consistency with the observed rainfall is very important.

Analyses of spatial distribution were performed on a daily basis and then accumulated to show the annual, seasonal, and monthly spatial distribution of rainfall. The spatial distribution of the annual (January 1 to December 31), monsoon, and winter season observed (gauge-observed) and CPC_RFE2.0 (satellite-estimated) rainfall means for each grid for each of the years from 2002 to 2007 are presented in Figures 10, 11, and 12.

The maps show a marked variation in both amount and spatial pattern between the estimated CPC_RFE2.0 rainfall and the observed annual values. The observed values show a generally decreasing trend in rainfall from east to west with numerous pockets of high rainfall. The CPC_RFE2.0 estimated values show a decreasing trend from south to north. The lowest observed rainfall is in an area around 83°45'E and 29°N, which is a trans-Himalayan rain shadow region north of the Annapurna Himalayan range. The observed values show a high rainfall area around Lumle (83°48'17"E and 28°17'53"N) in central Nepal which is not captured by the CPC_RFE2.0 at all, as was observed in a comparison with the GSMaP satellite product (Shrestha et al. 2011). The CPC_RFE2.0 actually indicates that the maximum rainfall is in the central south and far southwestern areas.

Around 70 per cent of the annual rainfall is in the monsoon season, thus the maps for this season are very similar to those for annual rainfall, except that the total amounts are slightly less (Figure 11).

The winter season maps (December, January, and February) are very different (Figure 12). In contrast to the annual and monsoon values, in many places, the CPC_RFE2.0 estimates are higher than the observed values, especially

Table 6: **Seasonal distribution of rainfall as observed by rain gauge (OBS) and satellite estimated (SRE) for 2002 to 2007 (all grids)**

	OBS				SRE			
	Season				Season			
Year	DJF	MAM	JJAS	ON	DJF	MAM	JJAS	ON
2002	108	274	1,311	45	118	197	725	94
2003	107	188	1,530	35	95	171	909	42
2004	58	252	1,269	94	49	149	818	47
2005	88	154	1,159	95	66	125	638	44
2006	17	265	1,130	48	11	179	729	32
2007	111	214	1,477	59	138	170	771	17
Mean	82	224	1,313	62	80	165	765	46

Figure 9: **Seasonal rainfall (in mm) as observed by rain gauge and satellite estimated for 2002 to 2007 (all grids)**

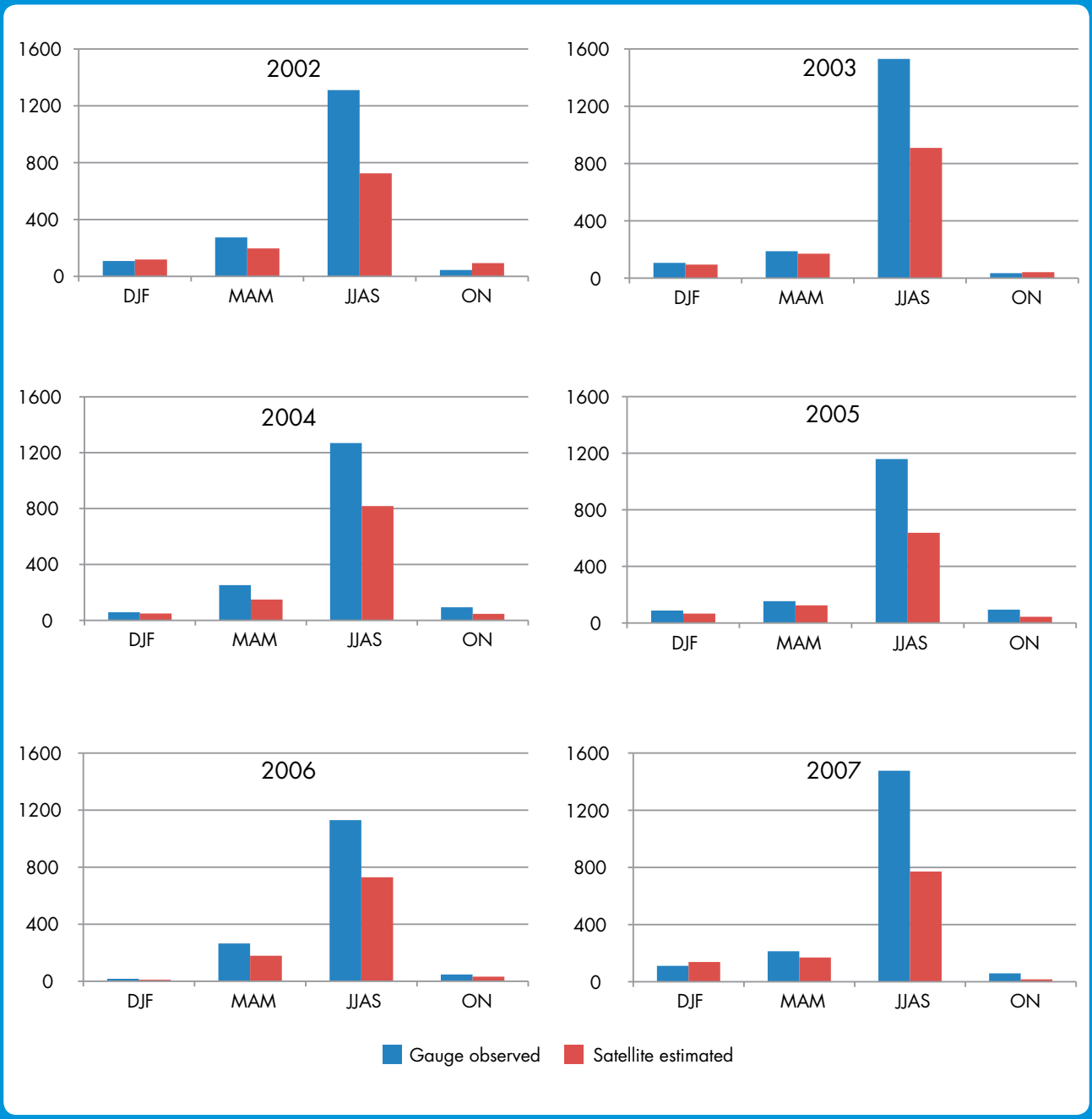

in the western part of Nepal. This means that the bias is less in this season and suggests that the application of bias correction for flood forecasting should be made with caution.

Monthly Bias Map Preparation and Analysis

A bias map provides information on whether the model predictions (in this case, the satellite-based estimates) are overestimated or underestimated. Bias maps were prepared for each month using the average daily observed and satellite-estimated rainfall values over all years from 2002 to 2007 (Figure 13). Red shading in the bias map indicates areas where the satellite-estimated values are higher than the observed rainfall values (positive bias); blue shading indicates areas where the satellite-estimated values are lower than the observed rainfall values (negative bias). The intensity of the colour reflects the extent of the over or underestimation. The values of the monthly total

Figure 10: **Spatial distribution of annual total rainfall (in mm) as observed by rain gauge (OBS) and satellite estimated (SRE) for 2002 to 2007 (all grids)**

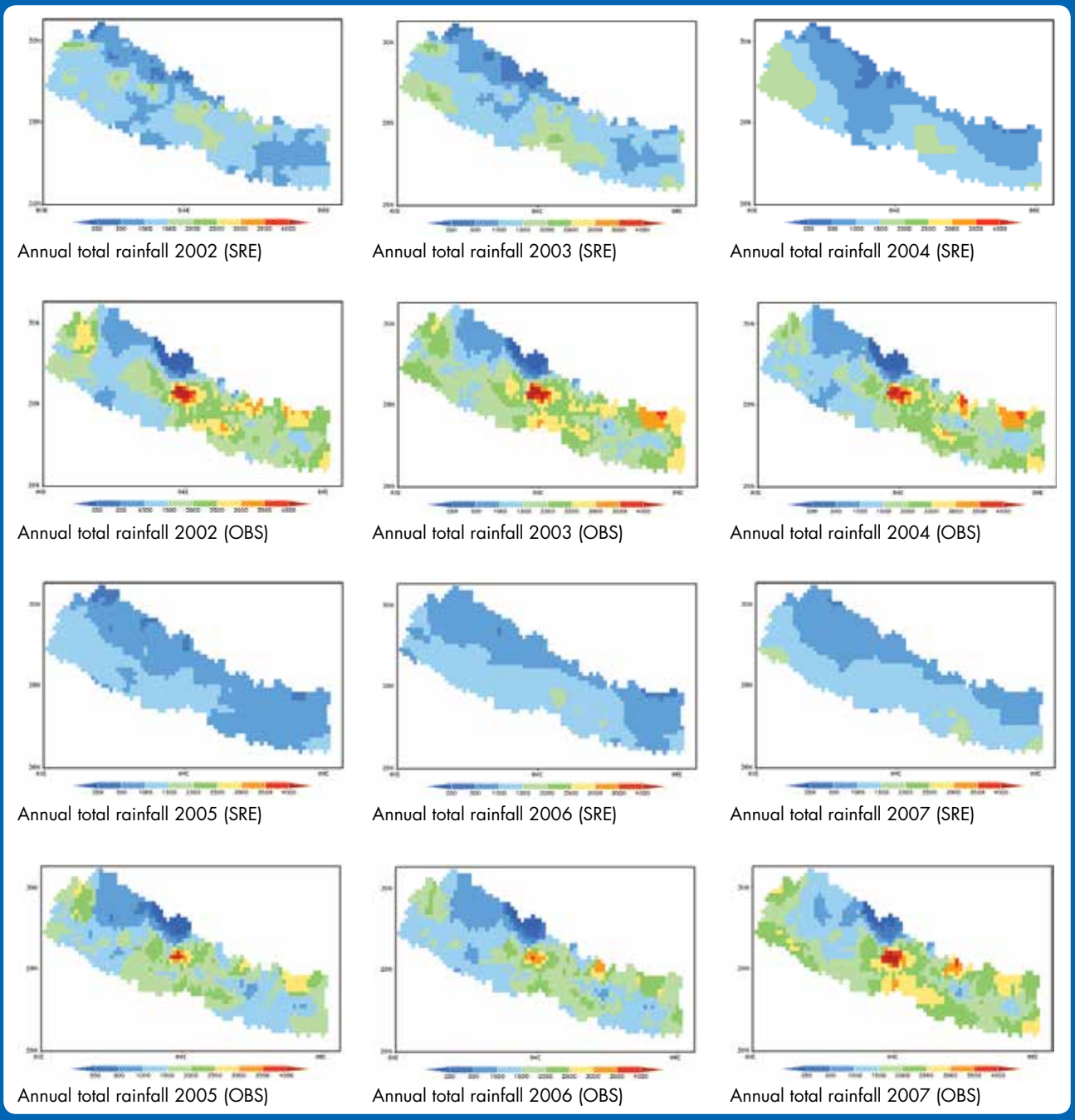

Annual total rainfall 2002 (SRE) | Annual total rainfall 2003 (SRE) | Annual total rainfall 2004 (SRE)

Annual total rainfall 2002 (OBS) | Annual total rainfall 2003 (OBS) | Annual total rainfall 2004 (OBS)

Annual total rainfall 2005 (SRE) | Annual total rainfall 2006 (SRE) | Annual total rainfall 2007 (SRE)

Annual total rainfall 2005 (OBS) | Annual total rainfall 2006 (OBS) | Annual total rainfall 2007 (OBS)

bias over the whole country for each year for 2002 to 2007 and the mean values for the whole period are given in Table 7.

Over all years, satellite estimation shows an average annual negative bias of 627 mm (Table 7). The satellite-estimated values show both positive and negative values at different places in all months, but with a negative bias on average in most months (Figure 13, Table 7). Overall, the negative bias is least in November and highest in July, and there is a small positive bias in December, January, and March. Throughout the year, there is marked positive bias over the rain shadow region in the Annapurna Himalayan range.

Figure 11: **Spatial distribution of total monsoon rainfall (in mm) as observed by rain gauge (OBS) and satellite estimated (SRE) for 2002 to 2007 (all grids)**

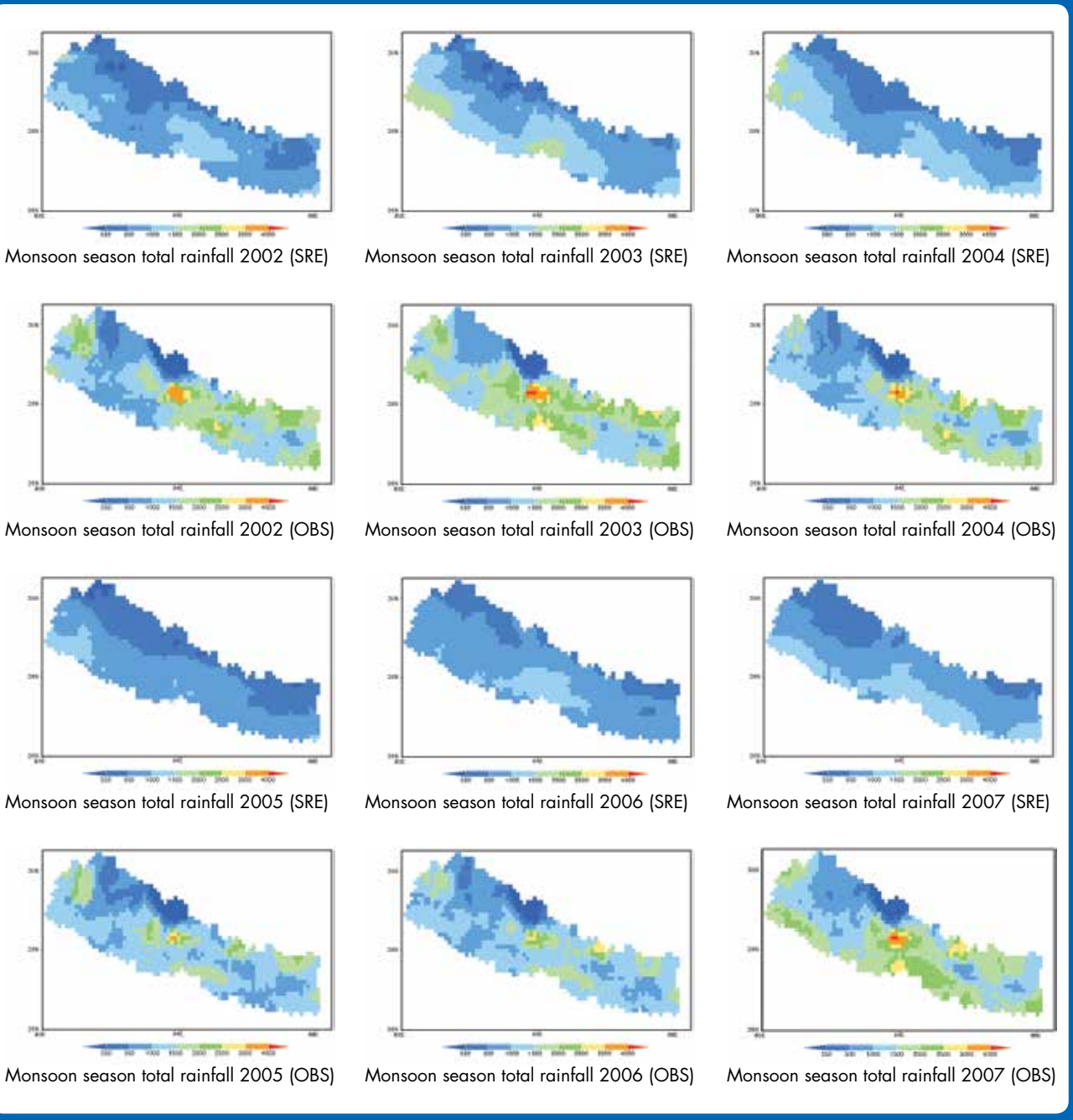

Monsoon season total rainfall 2002 (SRE) | Monsoon season total rainfall 2003 (SRE) | Monsoon season total rainfall 2004 (SRE)

Monsoon season total rainfall 2002 (OBS) | Monsoon season total rainfall 2003 (OBS) | Monsoon season total rainfall 2004 (OBS)

Monsoon season total rainfall 2005 (SRE) | Monsoon season total rainfall 2006 (SRE) | Monsoon season total rainfall 2007 (SRE)

Monsoon season total rainfall 2005 (OBS) | Monsoon season total rainfall 2006 (OBS) | Monsoon season total rainfall 2007 (OBS)

Table 7: **Monthly, six-year monthly mean, and annual total values of total bias (all grids) of satellite-estimated (CPC_RFE2.0) compared to observed rainfall values for 2002 to 2007**

Year	Jan	Feb	Mar	Apr	May	Jun	Jul	Aug	Sep	Oct	Nov	Dec	Total
2002	1	8	12	-1	-88	-61	-306	-131	-88	46	3	-2	**-607**
2003	0	-11	8	-3	-22	-172	-229	-136	-85	6	1	-5	**-646**
2004	-4	-1	-7	-23	-73	-47	-222	-87	-96	-40	-7	0	**-605**
2005	-22	0	8	-11	-27	-81	-172	-227	-41	-47	-3	-3	**-626**
2006	1	-5	-6	-34	-47	-60	-108	-123	-111	-15	-1	22	**-485**
2007	47	-42	-9	-1	-35	-152	-224	-211	-118	-37	-6	-3	**-791**
Average	**4**	**-8**	**1**	**-12**	**-49**	**-95**	**-210**	**-152**	**-90**	**-15**	**-2**	**2**	**-627**

Figure 12: **Spatial distribution of total winter season rainfall (in mm) as observed by rain gauge (OBS) and satellite estimated (SRE) for 2002 to 2007 (all grids)**

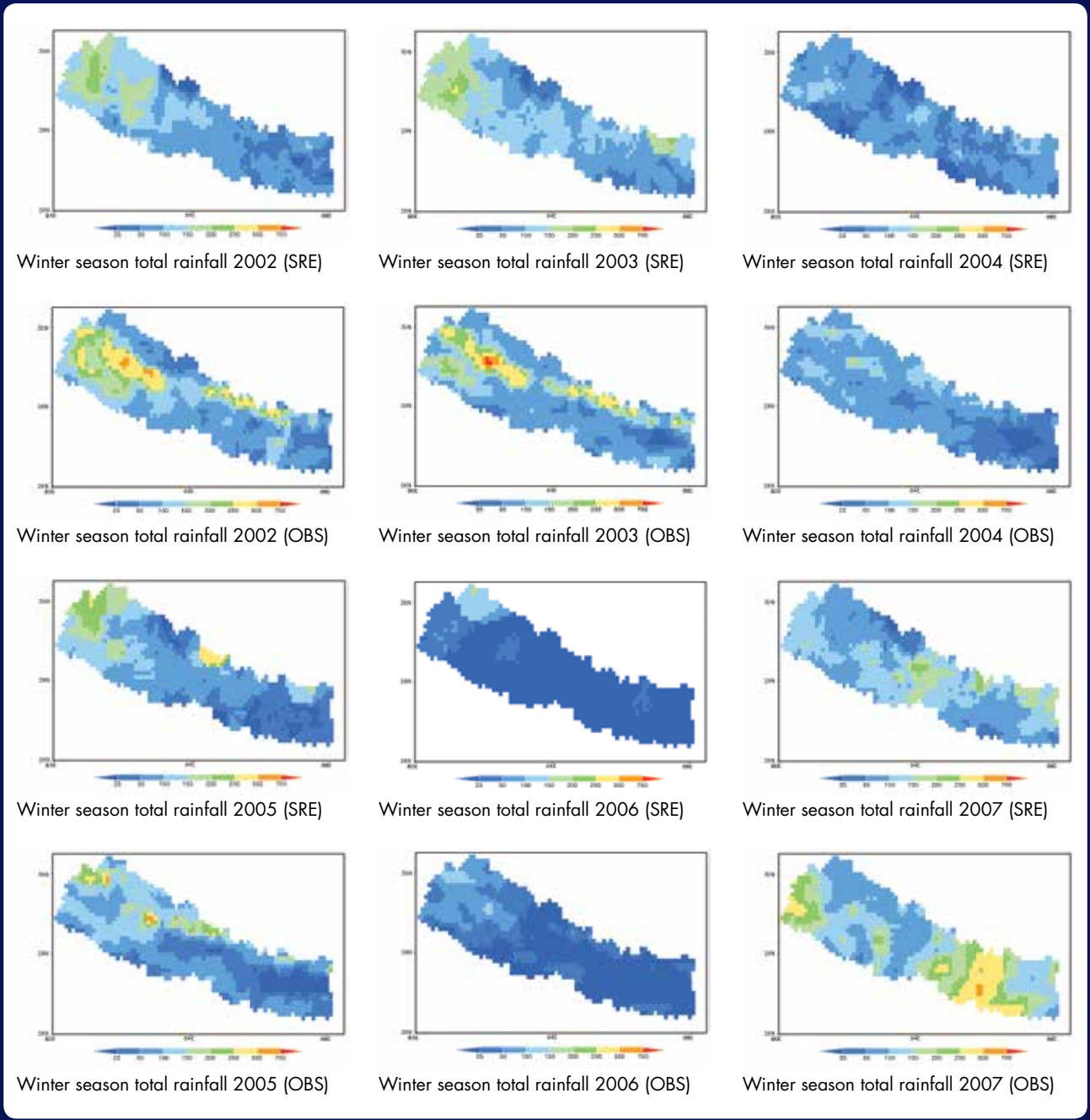

Error Statistics for Satellite-Based Rainfall Estimate

The overall error statistics for the satellite-estimated rainfall for the period from 2002 to 2007 derived from the daily satellite-estimated values are summarized in Table 8. The table shows the values for bias rainfall, root mean square error (RMSE), multiplicative bias, correlation coefficient, probability of detection (POD), false alarm ratio (FAR), threat score (TS), and equitable threat score (ETS). A contingency table was also derived through categorical analysis using a rainfall threshold value of 1 mm. Changing the threshold value might result in slight changes in the table.

The average daily rainfall bias is -1.72 mm. Accumulation of the bias over a year leads to an underestimation of more than 600 mm – a significant amount. Equally, there is a 72 per cent correlation between the observed and

Figure 13: **Monthly bias map between satellite-estimation (CPC_RFE2.0) and observed rainfall for the period from 2002 to 2007 based on daily average values**

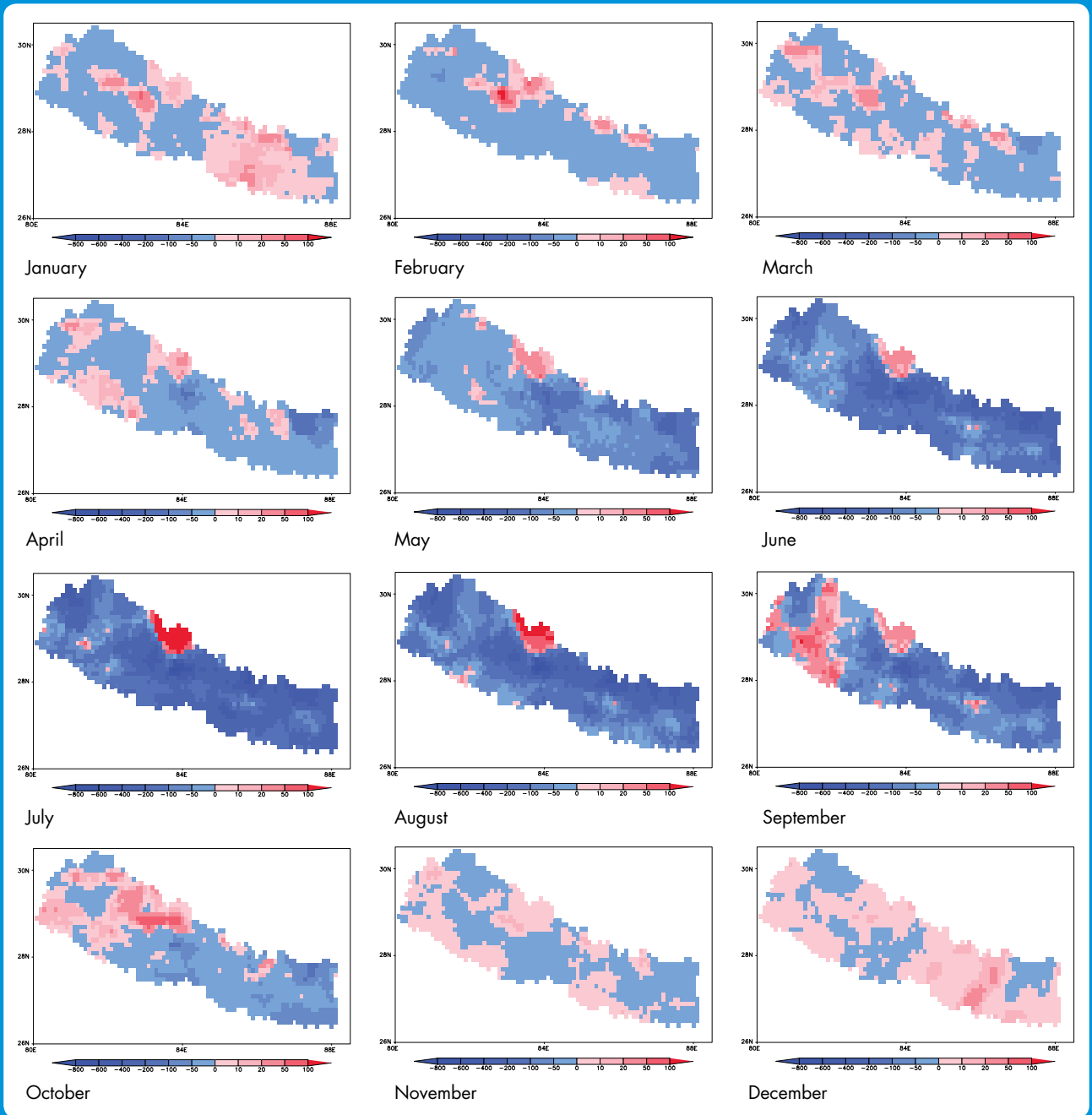

estimated values (Table 8). The probability of detection is also quite high (0.80) and the false alarm ratio (0.07) relatively low. This means that statistical bias correction could be applied to the data so that it could be used in flood forecasting.

Figure 14 shows scatter plots of observed rainfall against satellite-based estimates for each year from 2002 to 2007. The SRE estimations are lower than the observed values (slope<45°) and sometimes fail to capture higher rainfall values. These scattered values affect the average values.

Figure 14: **Scatter plots of observed and satellite-estimated rainfall from 2002 to 2007 based on grid-to-grid comparison**

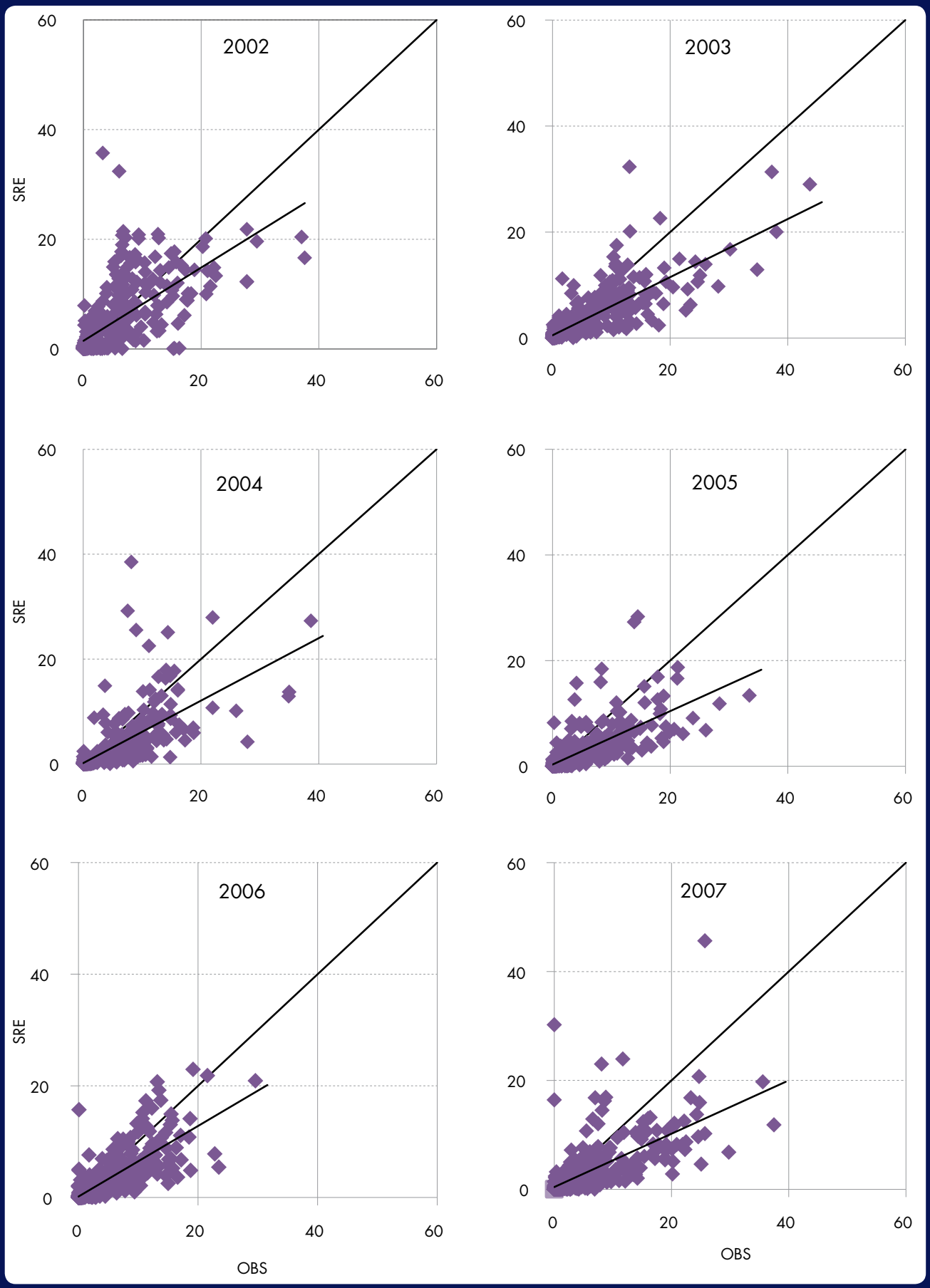

Table 8: **Annual error statistics for satellite-estimated rainfall from 2002 to 2007**

Year	Bias mm/day	RMSE	Multiplicative bias	Correlation coefficient	POD	FAR	TS	ETS
2002	-1.7	5.1	0.65	0.64	0.78	0.12	0.71	0.42
2003	-1.8	4.6	0.65	0.81	0.86	0.10	0.79	0.59
2004	-1.7	4.7	0.64	0.69	0.80	0.02	0.78	0.61
2005	-1.7	4.3	0.58	0.72	0.76	0.07	0.72	0.50
2006	-1.3	3.5	0.67	0.79	0.80	0.07	0.76	0.57
2007	-2.2	5.5	0.57	0.67	0.77	0.04	0.74	0.53
Average	-1.7	4.6	0.63	0.72	0.80	0.07	0.75	0.54

Discussion and Conclusion

Satellite-Estimated Values

The different comparisons of satellite-estimated and observed rainfall all show that the CPC_RFE2.0 underestimates strongly on an annual basis, with a calculated average annual deficit of 627 mm over the whole country. In the high rainfall area in and around Lumle, the difference exceeds 2,000 mm. As expected, this pattern is the same in the monsoon season. However, during the winter season there are more areas where the estimated rainfall is higher than observed. Overall, the lowest bias is found during the winter season, with the minimum negative bias in November, and a small positive bias in December, January, and March. As the monsoon approaches, the bias increases, reaching a maximum in July. There is no definite pattern in the bias map.

The daily bias rainfall was -1.72 mm, with a correlation coefficient of 0.72, root mean square error of 4.62 mm, and multiplicative bias of 0.63 when all the grids in the country were considered. When considering only those grids with stations, the bias was -1.90 mm, correlation coefficient 0.73, root mean square error 5.23 mm, and multiplicative bias 0.61. Thus there was little difference in bias regardless of whether all grids were used or only those that contained a station.

Improving Values

Since the annual bias is very high, the rainfall estimates need to be improved before they can be used in a model. There are two main ways to improve the estimation: applying a bias correction and improving the SRE algorithm.

Bias correction

The correlation and probability of detection values between the satellite-estimated and observed data were quite high, and the false alarm ratio was relatively low, thus in principle it is possible to apply a bias correction based on statistical analysis. Two methods were used to investigate the results of applying a bias correction. Bias corrections were calculated from the daily average rainfall from 2002 to 2007 and applied to the values for 2008. In the first method, the mean difference between the observed and estimated values was calculated for each grid and adjusted. In the second method, a ratio or multiplication factor was calculated for each grid and a correction was applied to those grids in which the rainfall amount was greater than a threshold value of 1.0 mm.

Figure 15 shows the observed (averaged), satellite-estimated, and two different bias corrected satellite-estimated values of annual total rainfall for 2008. Figures 16 and 17 show the maps for the monsoon and winter seasons separately. The annual and monsoon rainfall maps were significantly improved after the bias adjustments and show a much greater similarity to the map of observed values, with the greatest improvement using the ratio multiplied method. The amount of rainfall in the winter season is quite low and there was little difference between the estimated and observed values or the values following bias correction. Bias correction may not be needed in this season.

The accumulated monthly rainfall values for 2008 – observed, satellite-estimated, and after bias correction – are summarized in Table 9 and shown graphically in Figure 18. The rainfall values were significantly improved after bias adjustment, especially using the ratio multiplied method, but there is still a considerable discrepancy in the monsoon months, indicating the need for further research and study. One possibility that could be considered is that of developing a variable bias correction based on estimated rainfall amount.

Improving the algorithm

The algorithm used to derive the SRE data has not yet been fully optimized for use in the Himalayan region with its extreme variations in topography and rainfall. For example, at present the basic algorithm ignores GTS data when more than 200 mm is reported. But in the HKH region, there are many rainfall events in a year with more than 200 mm per day, and this restriction should be reviewed. Orographic effects are also not considered in the present SRE. The cloud top temperature in the algorithm could be reconsidered, as orography is always present in

Figure 15: **Spatial distribution of annual rainfall (in mm) in 2008** (a) rain-gauge-observed; (b) satellite estimated; (c) bias corrected satellite estimated (difference adjusted); and (d) bias corrected satellite estimated (ratio multiplied)

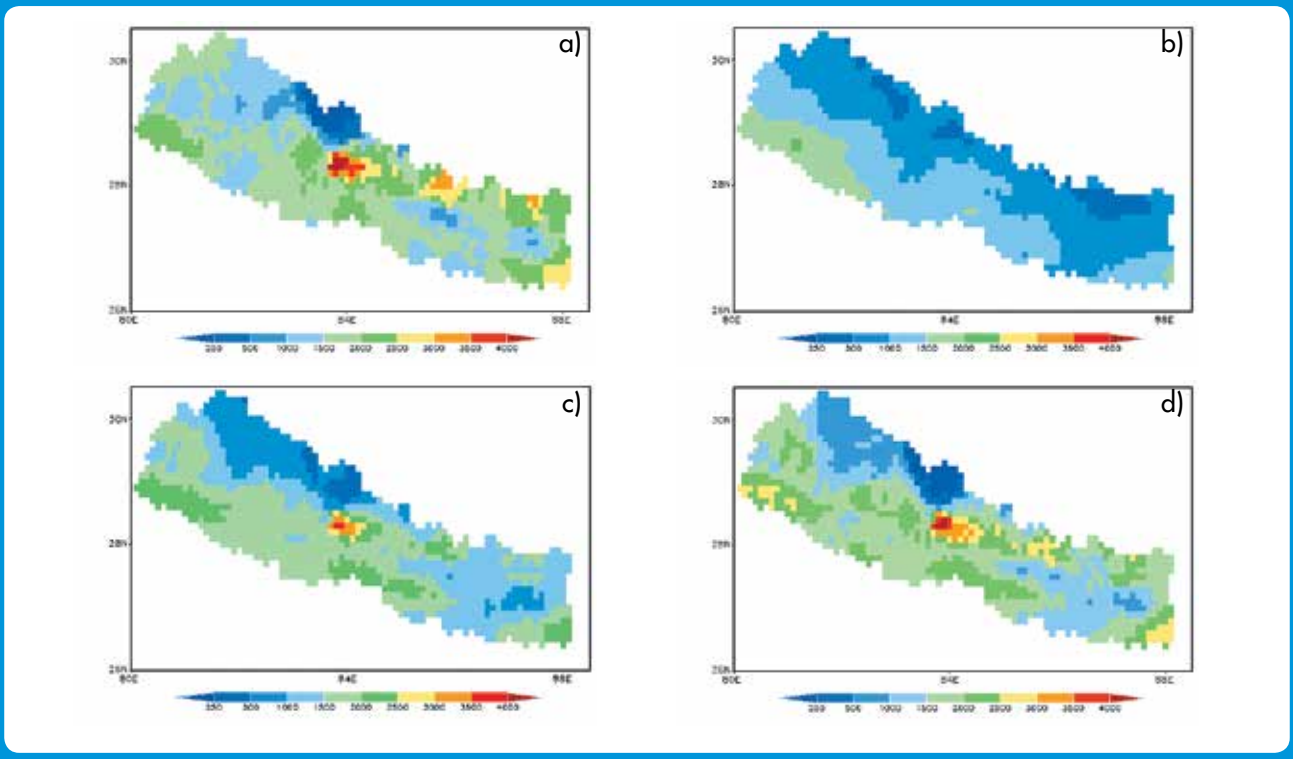

Figure 16: **Spatial distribution of monsoon rainfall (in mm) in 2008** (a) rain-gauge-observed; (b) satellite estimated; (c) bias corrected satellite estimated (difference adjusted); and (d) bias corrected satellite estimated (ratio multiplied)

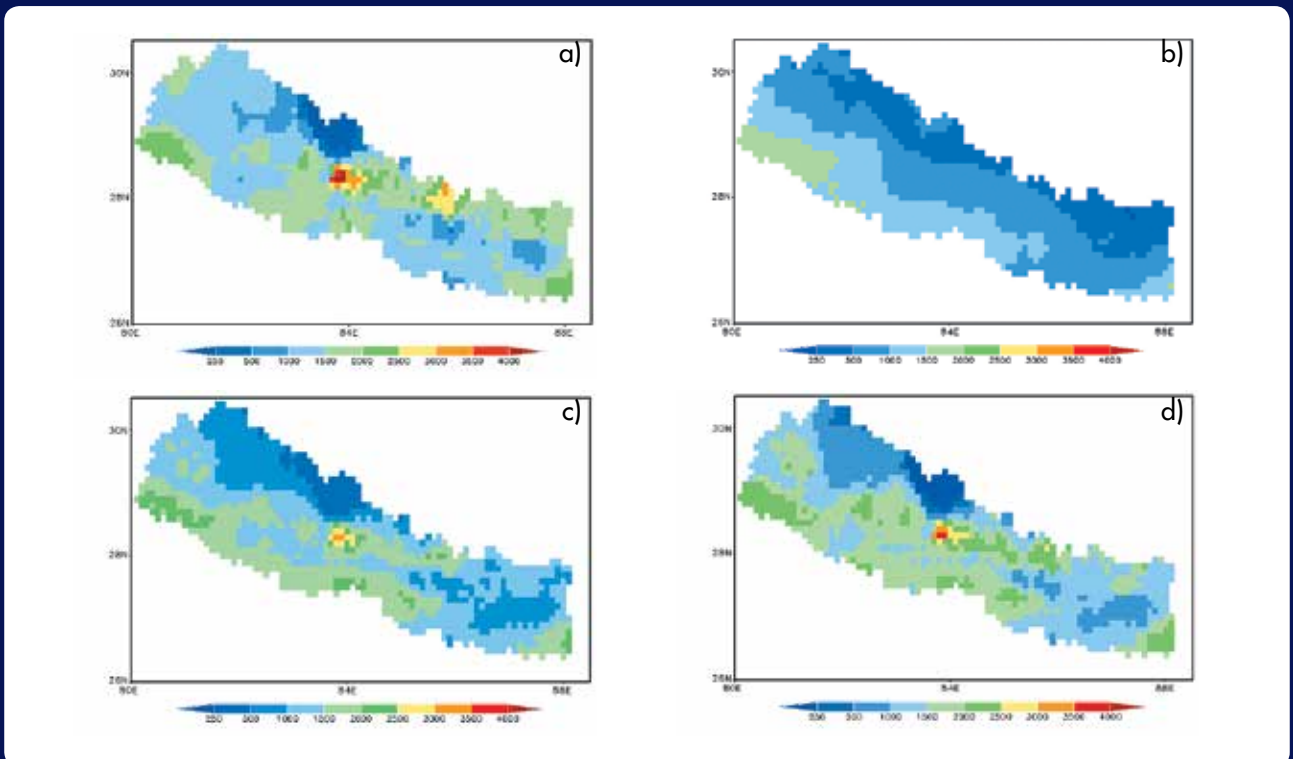

Table 9: **Monthly total observed and estimated rainfall in 2008 (mm)**

	Jan	Feb	Mar	Apr	May	Jun	Jul	Aug	Sep	Oct	Nov	Dec	Total
Rain-gauge-observed	10	4	17	48	116	372	427	429	210	31	1	0	1,664
CPC_RFE2.0 estimated	5	3	1	35	55	222	204	246	183	12	0	1	968
CPC_RFE2.0 estimated, bias corrected (difference adjusted)	7	4	1	38	86	312	368	387	218	17	0	0	1,438
CPC_RFE2.0 estimated, bias corrected (ratio multiplied)	13	3	4	33	112	400	376	423	215	35	0	1	1,616

Figure 17: **Spatial distribution of winter rainfall (in mm) in 2008** (a) rain-gauge-observed; (b) satellite estimated; (c) bias corrected satellite estimated (difference adjusted); and (d) bias corrected satellite estimated (ratio multiplied)

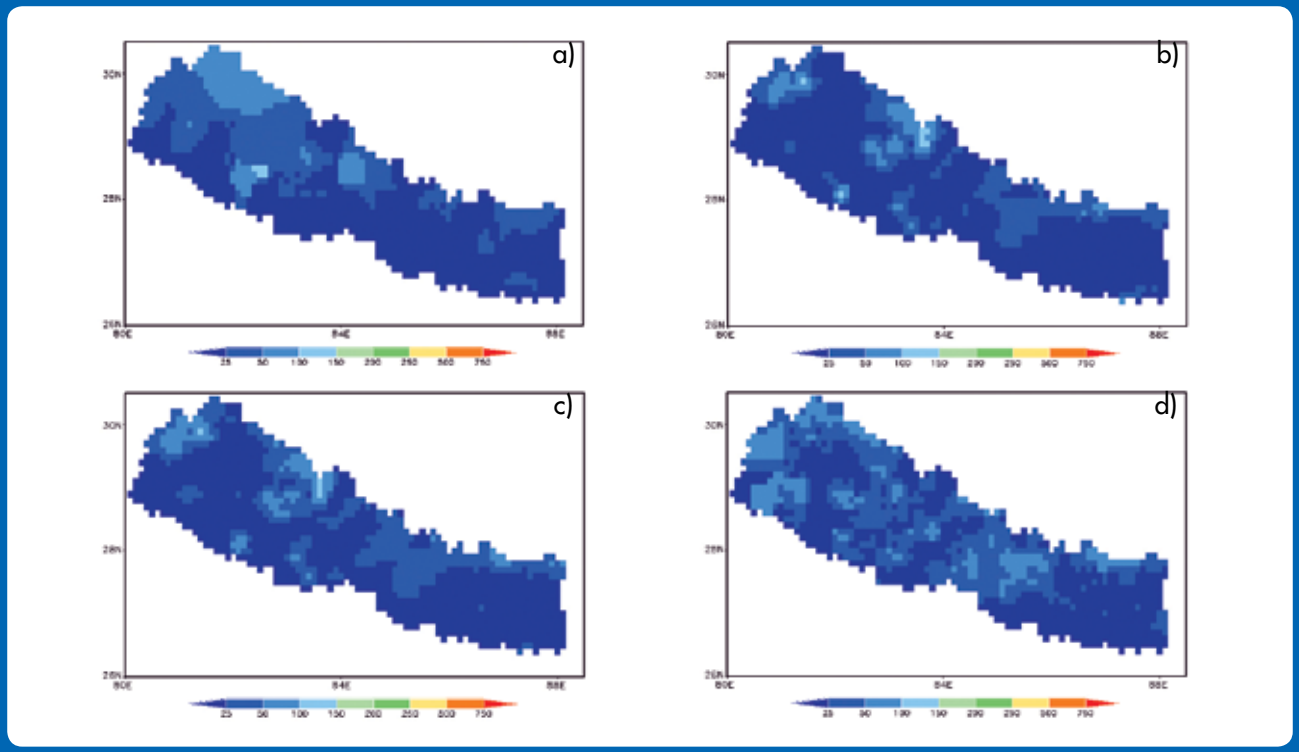

rainfall whether it is from the monsoon or western disturbances. Cloud top temperatures in orographic rain are greater than the threshold values in the present algorithm. The Nepalese Himalayas are always covered by snow, and it seems likely that the sensor is taking this as a cloud top temperature, especially during the winter season, and hence detecting rainfall. This may be one reason for the CPC_RFE2.0 values showing a decreasing trend from south to north and being higher than the observed values in rain shadow areas and during the winter period.

Figure 18: **Monthly total rainfall (in mm) for 2008**

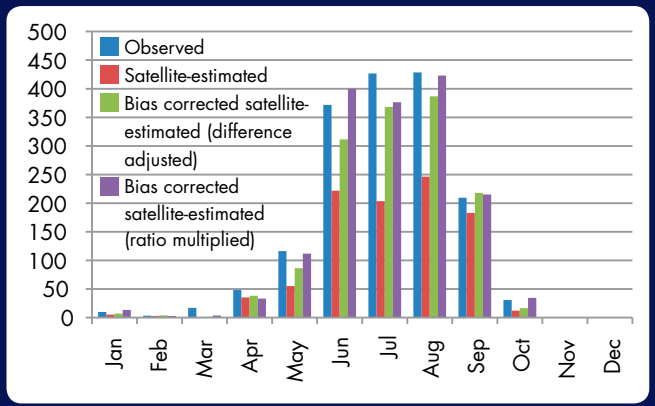

Conclusion

Nepal is a mountainous country, and it is extremely difficult to install and maintain rain gauges in remote areas where access is difficult. SRE can provide rainfall estimates for each pixel over a domain and thus has tremendous potential to provide data to support monitoring of flood and drought.

This assessment of the accuracy of the CPC_RFE2.0 indicates that the data need to be improved before they can be used in modelling. Ideally, the algorithm itself should be improved before being implemented. Now that one decade of SRE values are available, it may be possible to use the SRE climatology to improve the SRE algorithm. However, this tends to be a time-consuming process, and improvements in one area may disrupt other parts of the domain. Until a revised improved version of the CPC_RFE2.0 becomes available, we recommend that SRE bias correction (spatial and temporal) is applied before the results are used in further applications.

References

Adler, RF; Chang, GJ; Ferraro, R; Xie, P; Janowiak, J; Rudolf, B; Schneider, U; Curtis, S; Bolvin, D; Gruber, A; Susskind, J; Arkin, P; Nelkin, E (2003) 'The version-2 Global Precipitation Climatology Project (GPCP) monthly precipitation analysis (1979-present).' *J. Hydrometeorol*. 4: 1147–1167

Artan, GA; Gadain, H; Smith, JL; Asante, K; Bandaragoda, CJ; Verdin, JP (2007) 'Adequacy of satellite derived rainfall data for streamflow modelling.' *Nat. Hazards* 43: 167-185

Basistha, A; Arya, DS; Goel. NK (2007) 'Spatial distribution of rainfall in Indian Himalayas – A case study of Uttarakhand region.' *Water Resources Management* 22: 1325–1346. DOI 10.1007/s11269-007-9228-2

Clark, I (2001) Practical geostatics. Alloa, Scotland, UK: Geostokos Limited. www.kriging.com/PG1979/PG1979.pdf (accessed 26 February 2013)

Dinku, T; Chidzambwa, S; Ceccato, P; Connor, SJ; Ropelewski, CF (2008) 'Validation of high-resolution satellite rainfall products over complex terrain.' *Int. J. Remote Sens*. 29(14): 4097–4110

Ebert, EE (1996) *Result of the 3rd Algorithm Intercomparison Project (AIP-3) of the Global Precipitation Climatology Project (GPCP)*, Bureau of Meteorology Centre, Report No 55. Melbourne, Australia: Bureau of Meteorology Centre

Ebert, EE; Janowiak, JE; Kidd, C (2007) 'Comparison of near-real-time precipitation estimates from satellite observations and numerical models'. *Bull. Amer. Meteorol. Soc*. 88(1): 47–64

Hong, Y; Adler, RF; Negri, A; Huffman, GJ (2007) 'Flood and landslide applications of near real-time satellite rainfall estimation.' *Nat. Hazards* 43: 285–294

Huffman, GJ; Adler, RF; Bolven, DT; Gu, G; Nelkin, EJ; Bowman, KP; Hong, Y; Stocker, EF; Wolfe, DB (2007) 'The TRMM Multisatellite Precipitation Analysis (TMPA): Quasi-global, multiyear, combined-sensor precipitation estimates at fine scales.' *J. Hydrometeorol*. 8: 38–55

Isaaks, EH; Srivastava, RM (1989) *Applied geostatics*. Oxford, UK: Oxford University Press

Joyce, JJ; Janowiak, JE; Arkin, PA; Xie, P (2004) 'CMORPH: A method that produces global precipitation estimates from passive microwave and infrared data at high spatial and temporal resolution.' *J. Hydrometeorol*. 5: 487–503

Khanal, N; Shrestha, M; Ghimire, M (2007) *Preparing for flood disaster: Mapping and assessing hazard in the Ratu watershed*. Kathmandu, Nepal: ICIMOD

Kidd, C (2005) 'Validation of satellite rainfall estimates over the mid-latitudes.' In *Proceedings of the 2nd IPWG working group workshop, Monterey, CA*, 25-28 October 2004, pp 205-215. Monterey CA, USA: Naval Research Laboratory, Marine Meteorology Division, and Darmstadt, Germany: EUMETSAT

Kubota, T; Ushio, T; Shige, S; Kachi, M; Okamoto, K (2009) 'Verification of high resolution satellite-based rainfall estimates around Japan using a gauge-calibrated ground-radar dataset.' *J. Meteorol. Soc. Japan* 87A: 203–222

Laurent, H; Jobard, I; Toma, A (1998) 'Validation of satellite and ground based estimates of precipitation over the Sahel.' *Atmospheric Research* 47-48: 651-670

Shrestha, MS; Artan, GA; Bajracharya, SR; Sharma, RR (2008a) 'Applying satellite-based rainfall estimates for streamflow modelling in the Bagmati Basin, Nepal.' *J. Flood Risk Management* 1: 89–99

Shrestha, MS; Bajracharya, SR; Mool, P (2008b) *Satellite rainfall estimation in the Hindu Kush-Himalayan Region*. Kathmandu, Nepal: ICIMOD

Shrestha, MS; Takara, K; Kubota, T; Bajracharya, SR (2011) 'Verification of GSMaP rainfall estimates over the central Himalayas.' *Annual Journal of Hydraulics Engineering*, JSCE 55: 38-42

UNDP (2004) *Reducing disaster risk: A challenge for development*. New York: Bureau for Crisis Prevention and Recovery – United Nations Development Programme (BCPR-UNDP) www.preventionweb.net/english/professional/publications/v.php?id=1096 (accessed 26 February 2013

Ushio, T; Sasashige, K; Kubota, T; Shige, S; Okamota, K; Aonashi, K; Inoue, N; Takahashi, T; Iguchi, T; Kachi, M; Oki, R; Morimoto, T; Kawasaki, ZI (2009) 'A Kalman filter approach to the global satellite mapping of precipitation (GS_Map) from combined passive microwave and infrared radiometric data.' *J. Meteorol. Soc. Japan* 87A: 137–151

Vila, D; Scofield, R; Kuligowski, R; Davenport, J (2003) *Satellite rainfall estimation over South America: Evaluation of two major events*, NOAA Technical Report NESDIS 114. Washington DC, USA: U.S. Department of Commerce, National Oceanic and Atmospheric Administration

Vila, D; Lima, A (2006) 'Satellite rainfall estimation over South America: The hydroestimator technique.' In WW Grabowski (ed) *14th International Conference on Clouds and Precipitation, Bologna, Italy, 18–23 July 2004*. Amsterdam, Netherlands: Elsevier

Xie, P; Arkin, PA (1996) 'Analyses of global monthly precipitation using gauge observations, satellite estimates and numerical model predictions'. *J. Clim*. 9: 840–858

Xie, P; Yarosh, Y; Love, T; Janowiak, J; Arkin, PA (2002) 'A real-time daily precipitation analysis over South Asia.' *Preprints of the 16th Conference on Hydrology, Orlando, Florida*. Washington DC, USA: American Meteorological Society

Annex: Rain Gauge Stations

Details of the meteorological stations that provided the rain gauge data used in the study
(SN = serial number; StNo = Station number; LonDD = longitude; LatDD = latitude; Elev = elevation in masl).

SN	StNo	LonDD	LatDD	Elev
1	101	80.50	29.65	842
2	102	80.42	29.55	1,635
3	103	80.53	29.47	1,266
4	104	80.58	29.30	1,848
5	105	80.22	29.03	176
6	106	80.35	28.68	159
7	107	80.57	29.85	1,097
8	108	80.47	29.53	2,370
9	201	80.87	29.62	1,456
10	202	81.22	29.55	1,304
11	203	80.98	29.27	1,360
12	204	81.32	29.38	1,400
13	205	81.13	29.00	1,388
14	206	81.45	28.95	650
15	207	81.12	28.53	140
16	208	80.92	28.75	195
17	209	80.55	28.80	187
18	210	81.12	28.97	340
19	211	81.20	29.38	3,430
20	212	80.82	28.57	152
21	214	80.68	29.12	1,304
22	215	80.63	28.87	288
23	217	81.28	29.15	1,345
24	218	80.95	29.25	617
25	302	81.77	29.32	1,006
26	303	82.17	29.28	2,300
27	304	82.32	29.28	3,080
28	305	81.60	29.13	1,210
29	306	82.15	29.55	2,133
30	307	82.12	29.55	3,048
31	308	81.90	29.20	1,905
32	309	81.63	29.23	1,814
33	310	82.22	29.27	2,310
34	311	81.83	29.97	2,800
35	312	82.92	28.93	2,058
36	401	81.25	28.88	950
37	402	81.72	28.85	1,402
38	403	81.33	28.78	260
SN	StNo	LonDD	LatDD	Elev
39	404	82.20	28.70	1,231
40	405	81.27	28.65	225
41	406	81.62	28.60	720
42	407	82.12	28.02	235
43	408	81.35	28.17	215
44	409	81.57	28.10	190
45	410	81.58	28.78	610
46	411	81.10	28.43	129
47	412	81.72	28.27	135
48	413	81.70	28.35	510
49	414	81.90	28.05	226
50	415	81.35	28.43	200
51	416	81.62	28.07	144
52	417	81.35	28.38	200
53	418	82.28	28.98	2,000
54	419	81.78	28.03	195
55	420	81.67	28.10	165
56	501	82.63	28.60	1,560
57	504	82.63	28.30	1,270
58	505	82.87	28.10	823
59	507	82.12	28.22	698
60	508	82.30	28.13	725
61	509	82.50	28.05	725
62	510	82.53	27.70	320
63	511	82.17	28.38	1,457
64	512	82.28	28.30	885
65	513	82.20	28.63	910
66	514	82.48	28.63	2,100
67	515	82.50	28.05	634
68	601	83.72	28.78	2,744
69	604	83.70	28.75	2,566
70	605	83.60	28.27	984
71	606	83.65	28.48	1,243
72	607	83.60	28.63	2,384
73	608	83.88	28.82	3,609
74	609	83.57	28.35	835
75	610	83.88	29.05	3,465
76	613	83.75	28.18	1,720
77	614	83.70	28.22	891
78	615	83.10	28.40	2,273
79	616	83.22	28.60	2,530
80	619	83.73	28.40	2,742
81	620	83.65	28.03	700
82	621	83.40	28.38	1,160
83	622	83.57	28.15	1,740

SN	StNo	LonDD	LatDD	Elev
84	624	83.78	28.97	3,570
85	625	83.68	28.90	3,570
86	626	83.60	28.47	1,770
87	627	83.48	28.38	1,550
88	628	83.30	28.50	1,970
89	629	83.38	28.57	2,330
90	630	83.62	28.13	790
91	701	83.43	27.95	442
92	702	83.53	27.87	1,067
93	703	83.47	27.70	205
94	704	84.05	27.68	150
95	705	83.43	27.52	109
96	706	84.22	27.68	154
97	707	83.47	27.53	120
98	708	83.67	27.53	125
99	710	83.87	27.58	164
100	715	83.15	27.93	1,760
101	716	83.07	27.55	94
102	721	83.05	27.77	200
103	722	83.27	28.17	1,280
104	723	82.80	27.68	80
105	725	83.25	28.07	1,530
106	726	83.80	27.87	500
107	727	83.28	27.47	95
108	728	83.75	27.53	154
109	801	84.90	28.37	1,334
110	802	84.37	28.28	823
111	804	84.00	28.22	827
112	805	83.88	28.10	868
113	806	84.62	28.67	3,650
114	807	84.35	28.13	855
115	808	84.42	27.93	965
116	809	84.62	28.00	1,097
117	810	83.82	27.88	460
118	811	84.12	28.12	856
119	813	83.82	28.27	1,600
120	814	83.80	28.30	1,740
121	815	84.10	28.03	500
122	816	84.23	28.55	2,680
123	817	84.28	27.97	358
124	818	83.97	28.27	1,070
125	820	84.02	28.67	3,420
126	821	83.80	28.38	1,960
127	823	84.62	28.20	1,120
128	824	84.10	28.37	1,820

SN	StNo	LonDD	LatDD	Elev
129	826	83.77	27.98	750
130	827	84.13	27.87	660
131	829	83.75	28.27	1,000
132	830	83.78	28.27	1,160
133	832	83.92	28.08	1,432
134	833	85.00	28.48	3,300
135	834	84.28	28.77	4,100
136	902	84.42	27.62	256
137	903	84.53	27.58	270
138	904	85.13	27.55	1,706
139	905	85.08	27.60	2,314
140	906	85.05	27.42	474
141	907	85.00	27.28	396
142	909	84.98	27.17	130
143	910	85.17	27.18	244
144	911	84.97	27.07	115
145	912	85.38	27.02	152
146	915	85.15	27.62	1,530
147	918	84.87	27.00	91
148	919	85.17	27.42	1,030
149	920	84.82	27.55	274
150	921	85.00	27.03	140
151	922	85.30	26.77	90
152	923	85.02	26.92	109
153	925	84.98	27.43	332
154	927	84.43	27.67	205
155	1,001	85.38	28.28	1,900
156	1,002	84.82	28.05	518
157	1,004	85.17	27.92	1,003
158	1,005	84.93	27.87	1,420
159	1,006	85.87	27.87	2,000
160	1,007	85.25	27.80	2,064
161	1,008	85.62	27.80	1,592
162	1,009	85.72	27.78	1,660
163	1,015	85.20	27.68	1,630
164	1,016	85.60	27.95	2,625
165	1,017	85.57	27.87	1,550
166	1,018	85.57	27.78	845
167	1,020	85.65	27.70	1,365
168	1,022	85.40	27.58	1,400
169	1,023	85.72	27.63	710
170	1,024	85.55	27.62	1,552
171	1,025	85.63	27.92	1,240
172	1,027	85.90	27.78	1,220
173	1,028	85.75	27.57	633

SN	StNo	LonDD	LatDD	Elev
174	1,029	85.33	27.67	1,350
175	1,030	85.37	27.70	1,337
176	1,035	85.48	27.75	1,449
177	1,036	85.63	27.68	865
178	1,038	85.18	27.72	1,085
179	1,039	85.33	27.73	1,335
180	1,043	85.52	27.70	2,163
181	1,049	85.52	27.58	1,517
182	1,052	85.42	27.67	1,330
183	1,054	85.32	28.17	1,847
184	1,055	85.30	28.10	1,982
185	1,057	85.12	28.02	1,240
186	1,058	85.55	28.00	2,480
187	1,059	85.42	27.70	1,543
188	1,060	85.33	27.60	1,448
189	1,062	85.72	27.70	1,327
190	1,063	85.78	27.70	1,750
191	1,071	85.37	27.78	1,350
192	1,073	85.28	27.63	1,212
193	1,074	85.42	27.77	1,490
194	1,075	85.28	27.58	1,590
195	1,076	85.25	27.68	1,520
196	1,077	85.42	27.75	1,360
197	1,078	85.63	27.90	1,310
198	1,079	85.25	27.75	1,690
199	1,080	85.35	27.65	1,341
200	1,081	85.28	27.78	1,320
201	1,082	85.47	27.65	1,428
202	1,101	86.10	27.68	850
203	1,102	86.05	27.67	1,940
204	1,103	86.23	27.63	2,003
205	1,104	86.05	27.52	1,536
206	1,107	85.97	27.28	1,463
207	1,108	86.17	27.18	1,417
208	1,109	85.67	27.08	275
209	1,110	85.92	27.03	457
210	1,111	85.97	26.72	90
211	1,112	86.17	26.92	165
212	1,115	85.82	27.45	1,098
213	1,117	85.50	27.33	250
214	1,118	85.42	26.88	100
215	1,119	85.78	26.88	200
216	1,120	85.57	26.87	150
217	1,121	85.47	27.12	131

SN	StNo	LonDD	LatDD	Elev
218	1,122	85.78	26.65	172
219	1,123	86.08	27.47	495
220	1,202	86.72	27.70	2,619
221	1,203	86.57	27.43	1,982
222	1,204	86.75	27.35	2,143
223	1,206	86.50	27.32	1,720
224	1,207	86.42	27.48	1,576
225	1,210	86.43	27.13	497
226	1,211	86.83	27.03	1,295
227	1,212	86.93	26.73	100
228	1,213	86.52	26.93	1,175
229	1,215	86.43	26.73	138
230	1,216	86.22	26.65	102
231	1,219	86.58	27.50	2,378
232	1,222	86.80	27.22	1,623
233	1,223	86.75	26.55	91
234	1,224	86.38	27.55	1,662
235	1,226	86.90	26.60	85
236	1,301	87.28	27.55	1,497
237	1,303	87.33	27.28	1,329
238	1,304	87.28	27.05	1,680
239	1,305	87.28	27.13	410
240	1,306	87.23	27.03	1,317
241	1,307	87.35	26.98	1,210
242	1,308	87.33	26.93	365
243	1,309	87.15	26.93	143
244	1,311	87.28	26.82	444
245	1,312	87.38	26.62	152
246	1,314	87.55	27.13	1,633
247	1,316	87.17	26.82	183
248	1,317	87.42	27.77	2,590
249	1,319	87.27	26.48	72
250	1,320	87.27	26.70	200
251	1,321	87.22	27.28	303
252	1,322	87.17	26.97	158
253	1,325	87.15	27.37	1,190
254	1,326	87.50	26.73	250
255	1,399	87.27	27.62	2,100
256	1,403	87.78	27.55	1,780
257	1,405	87.67	27.35	1,732
258	1,406	87.93	27.20	1,830
259	1,407	87.90	26.92	1,300
260	1,408	87.70	26.67	163
261	1409	87.98	26.63	122

SN	StNo	LonDD	LatDD	Elev
262	1410	88.03	26.88	1,654
263	1412	88.05	26.57	120
264	1415	87.97	26.68	168
265	1416	88.07	26.87	1,678

SN	StNo	LonDD	LatDD	Elev
266	1419	87.75	27.15	1,205
267	1420	87.60	27.35	763
268	1421	87.90	26.58	143
269	1422	88.02	26.40	60

International Centre for Integrated Mountain Development
GPO Box 3226, Kathmandu, Nepal
Tel +977-1-5003222 **Fax** +977-1-5003299
Email info@icimod.org **Web** www.icimod.org

ISBN 978 92 9115 283 4